RAB-6.2 and the retromer regulate glutamate receptor recycling through a retrograde pathway

Donglei Zhang,[1] Nora R. Isack,[1] Doreen R. Glodowski,[1] Jie Liu,[3] Carlos Chih-Hsiung Chen,[1,2] X.Z. Shawn Xu,[3] Barth D. Grant,[2] and Christopher Rongo[1]

[1]The Waksman Institute, Department of Genetics; and [2]Department of Molecular Biology and Biochemistry; Rutgers, The State University of New Jersey, Piscataway, NJ 08854
[3]The Life Sciences Institute, University of Michigan, Ann Arbor, MI 48109

Regulated membrane trafficking of AMPA-type glutamate receptors (AMPARs) is a key mechanism underlying synaptic plasticity, yet the pathways used by AMPARs are not well understood. In this paper, we show that the AMPAR subunit GLR-1 in *Caenorhabditis elegans* utilizes the retrograde transport pathway to regulate AMPAR synaptic abundance. Mutants for *rab-6.2*, the retromer genes *vps-35* and *snx-1*, and *rme-8* failed to recycle GLR-1 receptors, resulting in GLR-1 turnover and behavioral defects indicative of diminished GLR-1 function. In contrast, expression of constitutively active RAB-6.2 drove the retrograde transport of GLR-1 from dendrites back to cell body Golgi. We also find that activated RAB-6.2 bound to and colocalized with the PDZ/phosphotyrosine binding domain protein LIN-10. RAB-6.2 recruited LIN-10. Moreover, the regulation of GLR-1 transport by RAB-6.2 required LIN-10 activity. Our results demonstrate a novel role for RAB-6.2, its effector LIN-10, and the retromer complex in maintaining synaptic strength by recycling AMPARs along the retrograde transport pathway.

Introduction

AMPA-type glutamate receptors (AMPARs) mediate much of the excitatory postsynaptic response at central nervous system synapses, and the regulated trafficking of AMPARs is a pivotal mechanism by which neurons regulate synaptic strength at excitatory synapses (Shepherd and Huganir, 2007; Henley et al., 2011). Once endocytosed into early endosomes, AMPARs can be sorted either into recycling pathways, which send them back to the plasma membrane, or into degradation pathways, which send them to the lysosome via multivesicular bodies (MVBs) and late endosomes. Recycling of previously endocytosed AMPARs from endosomal pools can occur through recycling endosomes (Gerges et al., 2004; Park et al., 2004; Hanley, 2010). Such regulated recycling is important for long-term potentiation, long-term depression, and homeostatic plasticity (Turrigiano, 2008; Kessels and Malinow, 2009; Makino and Malinow, 2009). Given the complex cell biological organization of the neuron,

it is likely that additional trafficking mechanisms determine AMPAR abundance and composition at the synapse.

Recycling also occurs through retrograde transport from early endosomes back to the Golgi followed by exit from the Golgi to the plasma membrane. The retrograde pathway is particularly important for the retrieval of Golgi residents, signaling molecule chaperones, and membrane receptors, and the pathway can also be subjugated by pathogens and their toxins (Bonifacino and Rojas, 2006; Bonifacino and Hurley, 2008; Johannes and Popoff, 2008; Pan et al., 2008; Lieu and Gleeson, 2011; Pfeffer, 2011). Surprisingly, little is known about retrograde transport in neurons, and it remains unknown whether synaptic proteins or neurotransmitter receptors, such as AMPARs, use the retrograde pathway.

Retrograde transport is mediated by the retromer complex, which is comprised of sorting nexins (Vps5–SNX1/2) and the VPS26–VPS29–VPS35 subcomplex (Bonifacino and Rojas, 2006; Bonifacino and Hurley, 2008; Johannes and Popoff, 2008). The retromer is found on long tubules that extend from the early

THE JOURNAL OF CELL BIOLOGY

endosome, where it shunts cargo away from the endosomal sorting complex required for transport (ESCRT) on the limiting membrane (Arighi et al., 2004; Carlton et al., 2004; Rojas et al., 2007). In the absence of retromer function, retrograde cargo is inadvertently sent down the degradation pathway by the ESCRT complex via MVBs (Arighi et al., 2004; Carlton et al., 2004). Members of the Rab6 small GTPase family of proteins also regulate retrograde transport, yet how the function of the Rab6 GTPases is integrated with that of the retromer is unclear (Echard et al., 2000; Mallard et al., 2002; Del Nery et al., 2006). A role for the retromer in AMPAR trafficking has not been described.

AMPARs also undergo regulated trafficking in the interneurons of *Caenorhabditis elegans*. *C. elegans* AMPARs are comprised of two subunits, GLR-1 and GLR-2, which function in the command interneurons where they transduce synaptic input from nose-touch mechanosensory neurons and govern overall locomotory behavior (Hart et al., 1995; Maricq et al., 1995; Mellem et al., 2002; Chang and Rongo, 2005). GLR-1 and GLR-2 AMPARs also promote spontaneous reversals in the direction of locomotion (Zheng et al., 1999). Mutants that lack AMPAR function or fail to transport and maintain AMPARs at synapses have reduced nose-touch mechanosensitivity and exhibit a depressed frequency of spontaneous reversals; thus, these behaviors correlate with AMPAR synaptic abundance (Burbea et al., 2002; Shim et al., 2004; Glodowski et al., 2005). Previous genetic approaches have identified the Rab-type small GTPases RAB-5, UNC-108/RAB-2, and RAB-10 as key regulators of AMPAR trafficking in *C. elegans* (Glodowski et al., 2007; Chun et al., 2008; Park et al., 2009), raising the possibility that GLR-1 AMPARs are regulated by additional Rabs.

To understand how neurons regulate AMPAR recycling, we tested different candidate *C. elegans* Rabs for their ability to regulate GLR-1 trafficking. Here, we show that RAB-6.2, together with the retromer complex, promotes the retrograde recycling of GLR-1–containing AMPARs. We show that *rab-6.2* mutants display defects in GLR-1 localization and behavior consistent with defects in retrograde transport. We show that RAB-6.2 is colocalized with LIN-10, a member of the Mint/X11 family (Whitfield et al., 1999; Glodowski et al., 2007), regulating GLR-1 retrograde transport through this interaction. We propose that neurons use the retrograde transport pathway to regulate the synaptic abundance of neurotransmitter receptors and that the Mint family of proteins is part of the retrograde transport machinery.

Results

RAB-6.2 regulates GLR-1 trafficking

To screen through multiple Rabs for candidates that regulate GLR-1 trafficking, we generated transgenes that express dominant-negative GDP-locked versions of Rabs while restricting their expression to postembryonic command interneurons by using the *glr-1* promoter. The trafficking of GLR-1 can be monitored using the *nuIs25[glr-1::gfp]* transgenic strain, which expresses a rescuing GLR-1::GFP chimeric receptor that is localized to the postsynaptic face of synapses (Rongo et al., 1998; Burbea et al., 2002). Individual GLR-1::GFP-containing synapses

can be observed as small (0.5–0.7 µm) puncta along the ventral cord dendrites in wild-type young adult animals (Fig. 1 B). Expression of a GDP-locked version of one of the Rabs we tested, *rab-6.2*, resulted in a dramatic decrease in the number and fluorescence intensity of GLR-1::GFP puncta compared with wild type (Fig. 1 C and not depicted). We obtained a mutant for the *rab-6.2* gene, *rab-6.2(ok2254)*, that contains a deletion of *rab-6.2* sequences, including the promoter, both "switch" domains, and the GTPase catalytic core, resulting in a likely molecular null (Fig. 1 A). We observed a significant decrease in the number and fluorescent intensity of GLR-1 puncta along the ventral cord dendrites of *rab-6.2(ok2254)* mutants (Fig. 1, D–F; and Fig. S1 A), indicating that RAB-6.2 is required for proper GLR-1 localization. We also examined the localization of a presynaptic protein, SNB-1 (synaptobrevin; Nonet et al., 1998) and observed no difference in GFP-labeled SNB-1 puncta in mutants compared with wild type (Fig. 1 E and Fig. S2, A and B), indicating that the defects in GLR-1 subcellular localization are not caused by gross defects in synapse formation along GLR-1–expressing interneurons.

GLR-1 can form either homomeric channels or heteromeric channels with GLR-2 (Mellem et al., 2002; Shim et al., 2004; Chang and Rongo, 2005; Emtage et al., 2009). We introduced a transgene expressing GFP::GLR-2 (Mellem et al., 2002) into *rab-6.2* mutants and found a similar number and intensity of ventral cord puncta compared with wild type (Fig. 1 E, Fig. S1 B, and Fig. S2, C and D). GLR-1 can also associate with the coreceptor STG-1 (Stargazin) and the CUB domain protein SOL-1 (Zheng et al., 1999; Wang et al., 2008). We examined STG-1::GFP and SOL-1::GFP in *rab-6.2* mutants and found their pattern of localization to be similar to that of wild type (Fig. S2, G–J). CNIH-2 (cornichon homologue 2) associates with mammalian AMPARs, modulating their gating properties (Schwenk et al., 2009; Kato et al., 2010; Shi et al., 2010). We thus generated a transgene, P$_{glr-1}$::cnih-2::gfp, containing *C. elegans* CNIH-2 sequences fused to GFP and driven by the *glr-1* promoter. We found that CNIH-2::GFP is localized to puncta along ventral cord dendrites (Fig. S1 C and Fig. S2, E and F), although at a lower number in *rab-6.2* mutants compared with wild type (Fig. 1 E). These results suggest that the function of RAB-6.2 is biased toward regulating the trafficking of GLR-1 homomeric channels and some, but not all, of the cofactors known to associate with *C. elegans* AMPARs.

A decrease in synaptic GLR-1::GFP should result in a decrease in GLR-1 function. We found that both the spontaneous reversal rate (Fig. 1 G) and the mechanosensitivity (Fig. 1 H) of *rab-6.2* mutants was significantly lower than that in wild type, indicating that a loss of endogenous GLR-1 function accompanies the drop in synaptic GLR-1 in these mutants. We also directly tested whether RAB-6.2 can influence endogenous GLR-1 channel activity. Glutamate-activated currents can be recorded from the interneuron AVA in whole-cell configuration (Mellem et al., 2002). We measured GLR-1–mediated currents elicited by the application of 1 mM glutamate (Ward et al., 2008), and we found that there was a significant reduction in current amplitude in *rab-6.2* mutants versus wild type when AVA was voltage clamped at −70 mV (Fig. 1 I and Fig. S1 D). The current–voltage
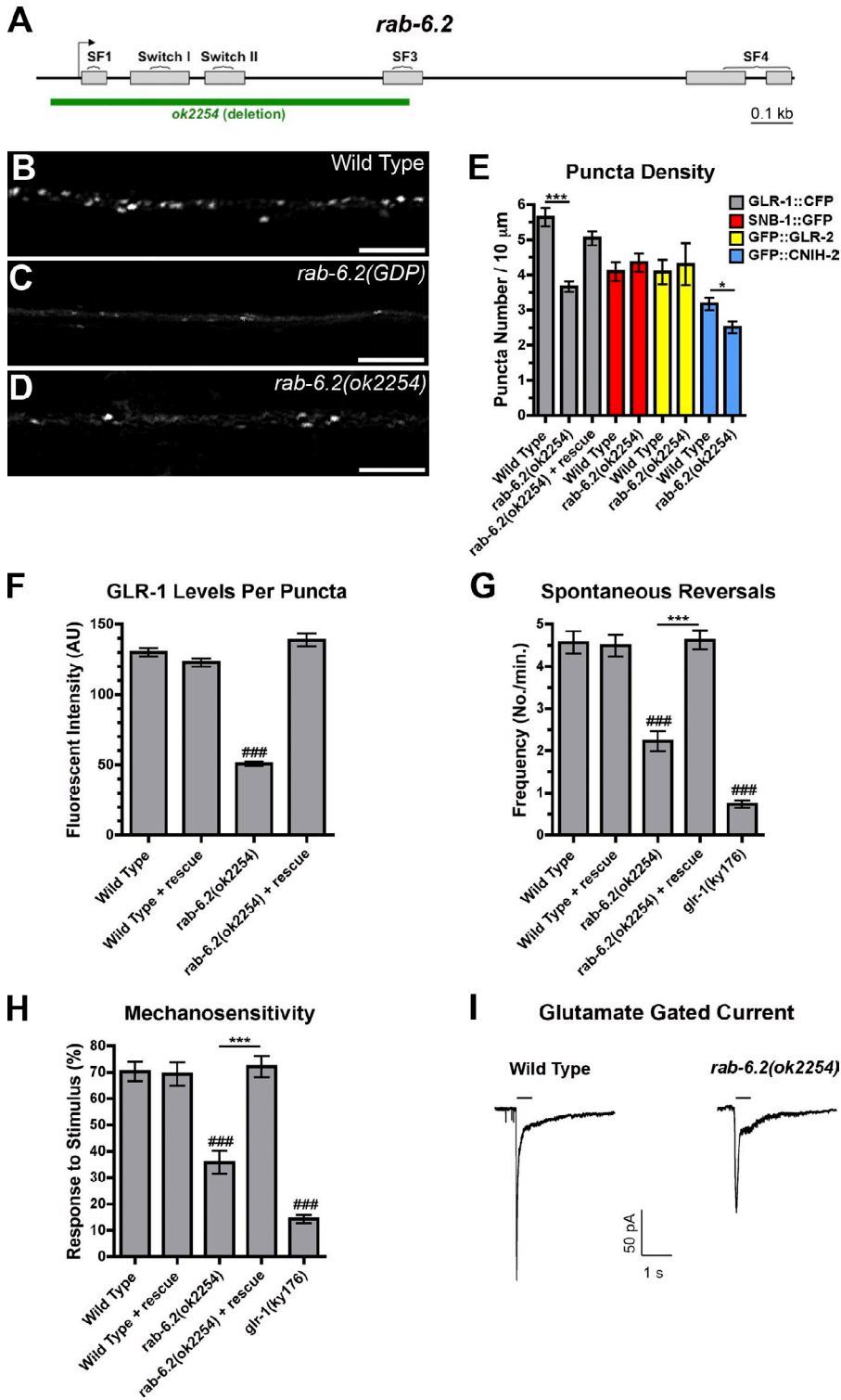
Figure 1. RAB-6.2 regulates GLR-1 trafficking. (A) Gene organization for *rab-6.2*. Gray boxes show exons. Brackets indicate regions encoding the indicated protein domains. The green line shows genomic DNA deleted in the *ok2254* mutant. (B–D) GLR-1::GFP fluorescence along dendrites of wild type (B), *rab-6.2(GDP)*–expressing mutants (C), and *rab-6.2(ok2254)* mutants (D). (E) Mean density of fluorescent puncta for the given reporter. (F) Mean fluorescent intensity of individual puncta. Rescue indicates animals that express a Venus::RAB-6.2 fusion protein via the *glr-1* promoter. (G) Mean spontaneous reversal frequency. (H) Mean nose-touch mechanosensory response. (I) Example of inward currents induced by glutamate application (bars) for a wild-type neuron and a *rab-6.2(ok2254)* mutant neuron. Bars, 5 µm. Error bars are SEM. *n* = 15–35 animals. Analysis of variance (ANOVA) with Dunnett's multiple comparison to wild type (###, P < 0.001) or Bonferroni multiple comparison test (*, P < 0.05; ***, P < 0.001). AU, arbitrary unit.

relationship in neurons from wild-type animals and *rab-6.2* mutants did not differ, indicating that *rab-6.2* mutants do not have general defects in conductance (Fig. S1, E–G).

RAB-6.2 regulates GLR-1 cell autonomously

To determine the expression pattern of RAB-6.2, we generated transgenes containing *rab-6.2* genomic sequences (including 2 kb of upstream promoter sequences, the complete ORF, and introns) fused in frame to GFP sequences. We introduced this *rab-6.2::gfp* transgene into nematodes and found that RAB-6.2::GFP is highly expressed in body wall muscles, pharyngeal and vulval muscles, hypodermis, intestine, the gonad, coelomocytes, and neurons (Fig. 2, A–I). We also introduced this transgene into nematodes that also express a P*glr-1*::*monomeric RFP* (*mRFP*) transgene (Shim et al., 2004), and we found that

Prab-6.2**::GFP**

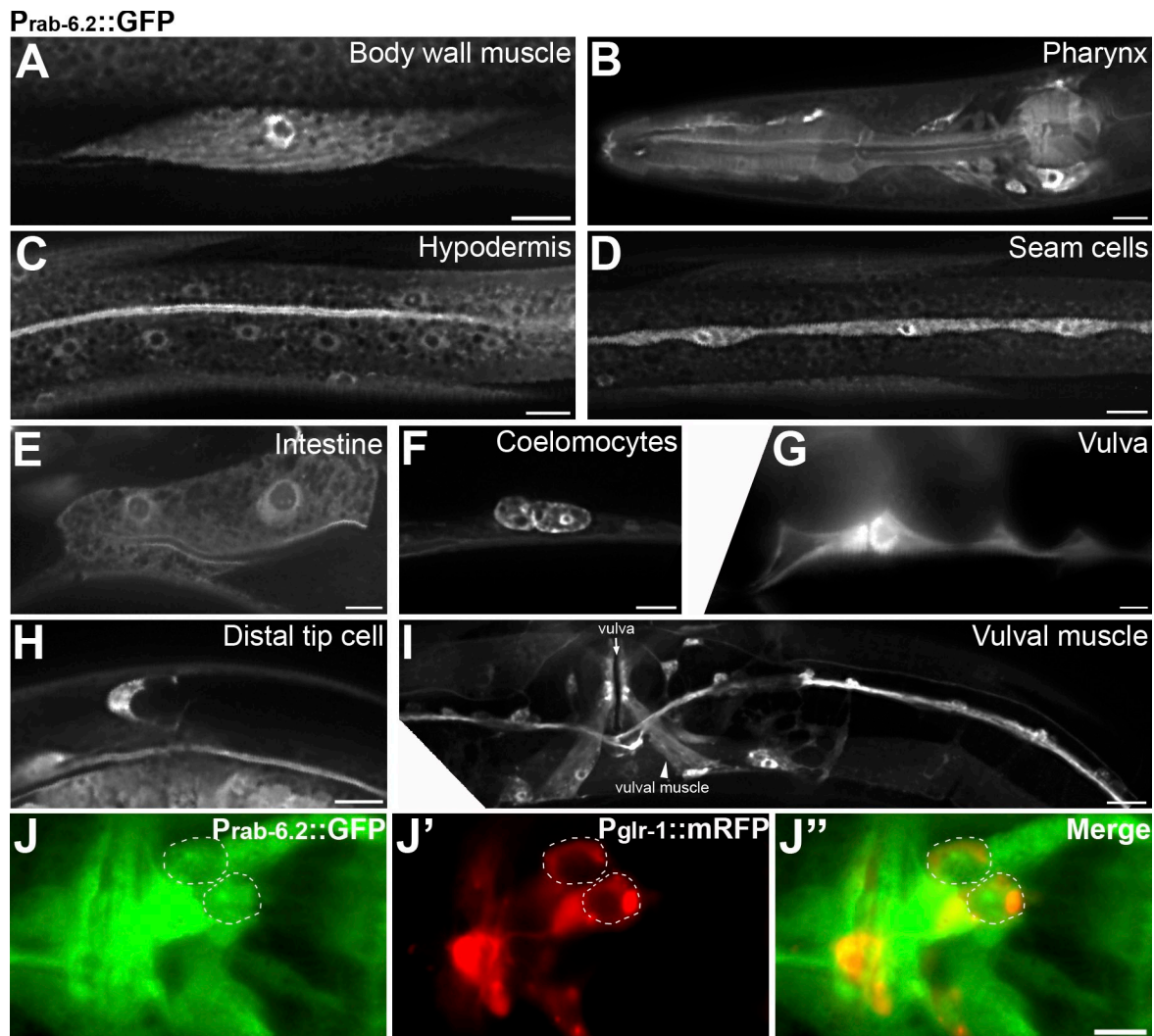|	
A Body wall muscle	**B** Pharynx
C Hypodermis	**D** Seam cells
E Intestine	**F** Coelomocytes / **G** Vulva
H Distal tip cell	**I** Vulval muscle (vulva / vulval muscle)
J Prab-6.2::GFP	**J'** Pglr-1::mRFP / **J''** Merge

Figure 2. **RAB-6.2 is broadly expressed in multiple tissues.** (A–I) Fluorescence from $P_{rab-6.2}::GFP$ in body wall muscles (A), pharyngeal muscle and head neurons (B), hypodermal cells (C), the seam cells (D), intestinal epithelia (E), coelomocytes (F), vulval epithelia (G), the distal tip cells (H), and the vulval muscles and ventral cord dendrites (I). (J–J'') Fluorescence from $P_{rab-6.2}::GFP$ (J) and $P_{glr-1}::mRFP$ (J') with images merged (J''). Coexpressing neurons are outlined. Bars, 5 µm.

RAB-6.2::GFP is expressed in the GLR-1–expressing command interneurons (Fig. 2 J).

To confirm that the *rab-6.2* gene is responsible for the mutant phenotypes and to test for the cell-autonomous function of RAB-6.2, we generated a transgene containing *glr-1* promoter sequences fused to *rab-6.2* cDNA sequences, with an N-terminal Venus to allow us to monitor expression and subcellular localization. We introduced this $P_{glr-1}::venus::rab-6.2$ transgene into wild-type animals and *rab-6.2* mutants, both of which express GLR-1::CFP (Chang and Rongo, 2005). We found that $P_{glr-1}::venus::rab-6.2$ completely rescued the defects in both GLR-1::CFP puncta number and puncta fluorescence intensity (Fig. 1, E and F) as well as the spontaneous reversal and mechanosensitivity defects (Fig. 1, G and H), indicating that RAB-6.2 functions cell autonomously.

RAB-6.2 regulates GLR-1 trafficking at a step after endocytosis

One explanation for the decrease in GLR-1::GFP puncta observed in *rab-6.2* mutants is that RAB-6.2 facilitates the retrograde transport of previously endocytosed GLR-1 receptors and that, in the absence of RAB-6.2 activity, these receptors are trafficked for degradation. We tested this model by determining whether endocytosis is required for the receptor turnover that we observe in *rab-6.2* mutants, as mutations that block GLR-1 endocytosis should suppress *rab-6.2*. The clathrin adaptin AP180 orthologue UNC-11 is a key mediator of GLR-1 endocytosis, and loss-of-function mutations in *unc-11* suppress the turnover and/or internal accumulation of receptors observed in membrane-recycling mutants (Nonet et al., 1999; Burbea et al., 2002). We analyzed GLR-1::GFP localization in *rab-6.2; unc-11* double mutants and found that mutations in *unc-11* prevent the decrease in GLR-1::GFP puncta number and fluorescence intensity observed in *rab-6.2* mutants (Fig. 3, A, B, and E; and Fig. S1 A). GLR-1 endocytosis is also facilitated by the direct ubiquitination of four key lysine residues on the C-terminal tail sequences of the receptor itself (Burbea et al., 2002). The *nuIs108[P_{glr-1}::glr-1(4kr)::gfp]* transgene expresses a GLR-1:: GFP in which the ubiquitinated lysines are mutated to arginines,
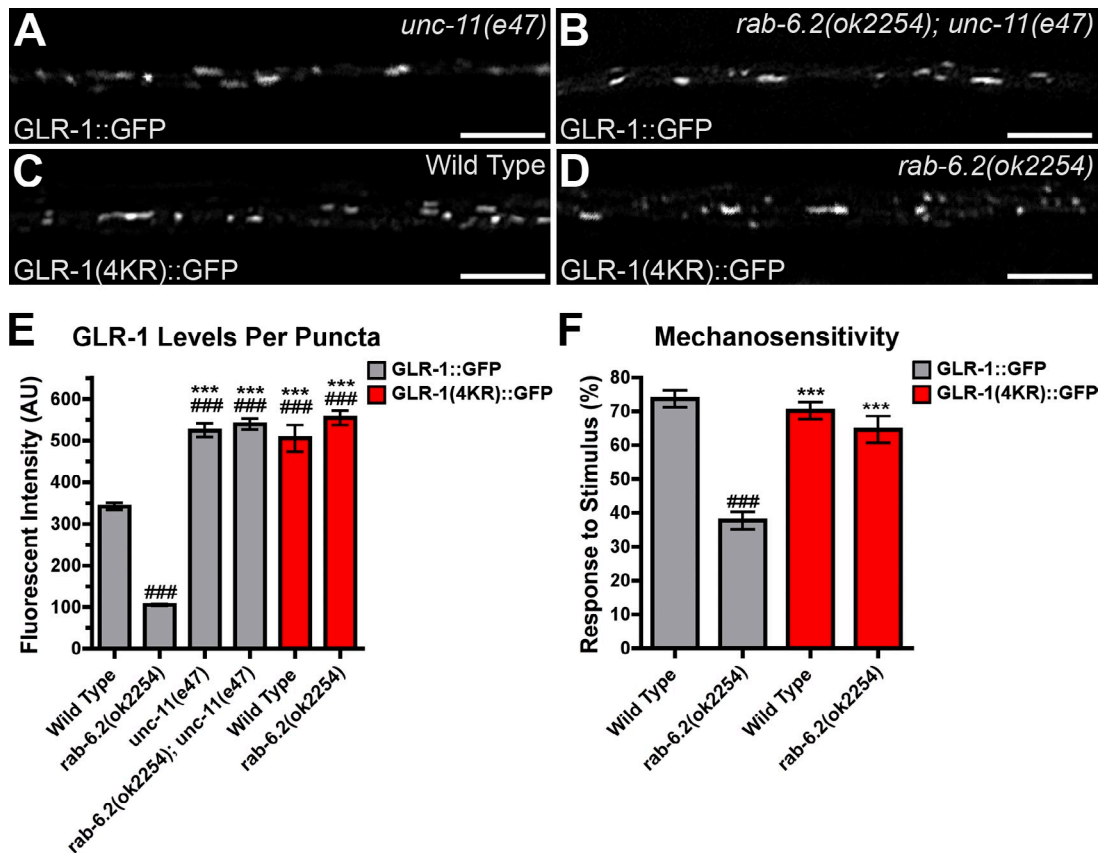
Figure 3. RAB-6.2 functions downstream of GLR-1 endocytosis. (A and B) GLR-1::GFP fluorescence in *unc-11(e47)* (A) and *rab-6.2(ok2254); unc-11(e47)* (B) mutants. (C and D) The fluorescence of GLR-1(4KR)::GFP in wild type (C) and *rab-6.2(ok2254)* mutants (D). (E) Mean fluorescent intensity (AU, arbitrary units) of puncta for the given reporter. (F) Mean nose-touch response. Bars, 5 μm. Error bars are SEM. *n* = 15–35 animals. ANOVA with Dunnett's multiple comparison to wild type (###, P < 0.001) or *rab-6.2(ok2254)* mutants expressing GLR-1::GFP (***, P < 0.001).

thereby precluding ubiquitination and depressing receptor endocytosis and turnover. Unlike for wild-type GLR-1::GFP, GLR-1(4KR)::GFP puncta number and fluorescence intensity is not altered in *rab-6.2* mutants compared with wild type (Fig. 3, C–E; and Fig. S1 A). Moreover, expression of GLR-1(4KR)::GFP, but not wild-type GLR-1::GFP, restored mechanosensitivity to *rab-6.2* mutants (Fig. 3 F). Our results indicate that clathrin-mediated endocytosis and receptor ubiquitination are required for the turnover of the GLR-1 receptor and loss of GLR-1 synaptic function observed in *rab-6.2* mutants, suggesting that RAB-6.2 regulates GLR-1 trafficking at a step after endocytosis and receptor ubiquitination.

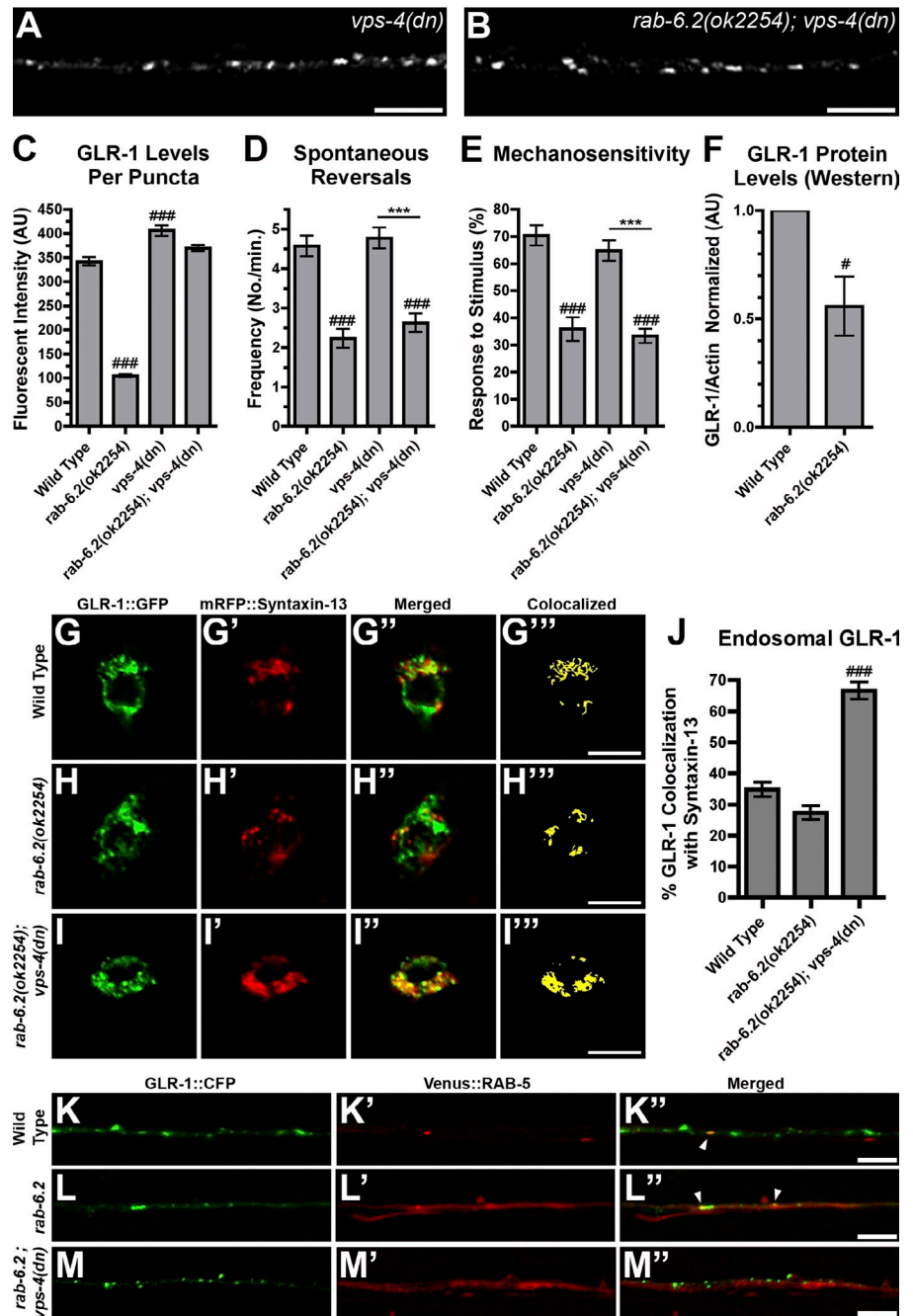### RAB-6.2 regulates the exit of GLR-1 from endosomes and GLR-1 turnover

The increase in GLR-1::GFP turnover observed in *rab-6.2* mutants suggested that GLR-1 might be improperly sorted from early endosomes to MVBs, late endosomes, and eventually lysosomes via ESCRT-mediated transport. We tested this possibility by blocking ESCRT-mediated transport in *rab-6.2* mutants and observing whether GLR-1 would accumulate in endosomes. The VPS-4 AAA ATPase facilitates the movement of endocytosed cargo from early endosomes to MVBs, and expression of a dominant-negative VPS-4 mutant protein can significantly reduce trafficking from early endosomes to MVBs

and the late endosome (Babst et al., 2002; Yeo et al., 2003). Neuronal expression of dominant-negative VPS-4 from the transgene *nuIs145[P$_{glr-1}$::vps-4(dn)]* blocks the movement of GLR-1 receptors from early endosomes to MVBs and decreases their ubiquitin-mediated turnover (Chun et al., 2008). We found that expression of dominant-negative VPS-4 in *rab-6.2* mutants restored GLR-1::GFP puncta number and fluorescence intensity to wild-type levels (Fig. 4, A–C; and Fig. S1 A), indicating that the ESCRT pathway is required for GLR-1 turnover when retrograde transport is blocked. Consistent with this model, we detected lower levels of GLR-1 in *rab-6.2* mutants by Western blotting in whole-nematode lysates (Fig. 4 F).

If the pathways for retrograde recycling and transport to MVBs are both blocked, GLR-1 should eventually accumulate in early endosomes and thus decrease synaptic GLR-1 function. We therefore measured the spontaneous reversal rate and mechanosensitivity of *rab-6.2* mutants compared with *rab-6.2* mutants that also express dominant-negative VPS-4. Although dominant-negative VPS-4 can prevent GLR-1 turnover, it cannot restore either the decreased frequency in reversal rates (Fig. 4 D) or the decreased mechanosensitivity (Fig. 4 E) observed in *rab-6.2* mutants, suggesting that the GLR-1 receptors in *rab-6.2 nuIs145[P$_{glr-1}$::vps-4(dn)]* animals are not accumulating at synaptic sites.

To determine the specific site of GLR-1 accumulation in these animals, we used the endosomal markers SYN-13

Figure 4. **RAB-6.2 regulates the exit of GLR-1 from endosomes.** (A and B) GLR-1::GFP fluorescence in dendrites of *vps-4(dn)* (A) and *rab-6.2(ok2254); vps-4(dn)* (B) mutants. (C–E) Mean fluorescent intensity of GLR-1 puncta (C), spontaneous reversal frequency (D), and nose-touch response for the indicated genotypes (E). (F) Total GLR-1 protein levels, normalized to actin, as detected in four independent Western blots. (G–I''') GLR-1::GFP (G–I) and mRFP::SYN-13 (G'–I') fluorescence in neuron cell bodies from wild type (G–G'''), *rab-6.2(ok2254)* (H–H'''), and *rab-6.2(ok2254); vps-4(dn)* (I–I''') mutants. (G''–I'') Merged images. (G'''–I''') Binary masks indicate colocalization by highlighting pixels with matching intensity values. (J) Mean percentage of GLR-1::GFP colocalized with endosomal marker mRFP::SYN-13, normalized to total GLR-1::GFP in cell bodies. (K–M'') GLR-1::CFP (K–M) and Venus::RAB-5 (K'–M') fluorescence along ventral cord dendrites from wild type (K–K''), *rab-6.2(ok2254)* (L–L''), and *rab-6.2(ok2254); vps-4(dn)* (M–M'') mutants. (K''–M'') Merged images. Arrowheads indicate colocalized puncta. Bars, 5 μm. Error bars are SEM. n = 15–35. ANOVA with Dunnett's multiple comparison to wild type (###, P < 0.001; #, P < 0.05) or Bonferroni multiple comparison test (***, P < 0.001). AU, arbitrary unit.

(syntaxin 13) and RAB-5. We observed mRFP::SYN-13 and GLR-1::GFP colocalization in neuron cell bodies as previously described (Chun et al., 2008; Park et al., 2009). We coexpressed mRFP::SYN-13 with GLR-1::GFP in both *rab-6.2* and *rab-6.2 nuIs145[P_{glr-1}::vps-4(dn)]* animals. Although we did not see a significant change in the amount of GLR-1::GFP colocalized with mRFP::SYN-13 puncta in *rab-6.2* mutants (∼30%; Fig. 4, G, H, and J), we found that the mRFP::SYN-13–labeled structures are increased in size, with nearly 70% of GLR-1::GFP colocalized, in *rab-6.2* mutants when MVB trafficking is blocked by dominant-negative VPS-4 (Fig. 4, I and J). We also coexpressed GLR-1::CFP with Venus::RAB-5 in both *rab-6.2* and *rab-6.2 nuIs145[P_{glr-1}::vps-4(dn)]* animals. In wild-type animals, Venus::RAB-5 is localized to a small number of puncta along the ventral cord dendrites, and a small number of GLR-1::CFP puncta colocalized with these Venus::RAB-5 puncta (Fig. 4 K). In *rab-6.2* mutants, Venus::RAB-5 becomes distributed throughout the dendrites, consistent with an enlargement of early endosomes caused by arrested retrograde transport (Fig. 4 L). The remaining GLR-1::CFP in *rab-6.2* mutants is colocalized with Venus::RAB-5, and this colocalization is also observed when MVB trafficking is blocked by dominant-negative VPS-4 (Fig. 4, L and M). Collectively, these results indicate that RAB-6.2 regulates the exit of endocytosed GLR-1 receptors out of early endosomes in neurons.

RAB-6.2 associates with GLR-1 and Golgi

To examine RAB-6.2 subcellular localization, we generated transgenes containing the *glr-1* promoter sequences fused to sequences encoding GFP, Cerulean, or Venus fused in frame to the N-terminal sequences of RAB-6.2. We found that RAB-6.2 is localized to punctate structures in the neuron cell body and along the ventral cord dendrites. We introduced the P_{glr-1}::*cerulean::rab-6.2* transgene into nematodes that express the Golgi resident protein mannosidase (MANS)::YFP (Rolls et al., 2002; Glodowski et al., 2005) and observed nearly complete colocalization between Cerulean::RAB-6.2 and MANS::YFP, indicating that RAB-6.2 is localized on or near Golgi structures (Fig. 5 A). We introduced the P_{glr-1}::*venus::rab-6.2* transgene into nematodes expressing GLR-1::CFP, and we found that GLR-1::CFP and Venus::RAB-6.2 are colocalized at or near individual puncta in both the cell body (Fig. 5 B) and the ventral cord dendrites (Fig. 5 C). Our results indicate that a minority of RAB-6.2 and GLR-1 puncta are colocalized, consistent for a cargo molecule and a specific Rab GTPase regulator of its trafficking.

To test whether a guanine nucleotide-bound state regulates RAB-6.2 subcellular localization, we introduced either GDP-locking (RAB-6.2(GDP), mutation T24N) or GTP-locking (RAB-6.2(GTP), mutation Q69L) mutations into the GFP-tagged transgene. Whereas wild-type GFP::RAB-6.2 is found in puncta along dendrites (Fig. 5 D), GFP::RAB-6.2(GDP) was diffusely distributed in the dendrites and cell body cytosol (Fig. 5 E and not depicted). In contrast, we found GFP::RAB-6.2(GTP) in a punctate pattern, with higher levels of punctate fluorescence intensity than those observed for the wild-type GFP::RAB-6.2 protein (Fig. 5 F). Thus, activation of RAB-6.2 by GTP binding results in its punctate localization.

RAB-6.2 can drive GLR-1 retrograde transport back to soma Golgi

To test whether the activation of RAB-6.2 has an instructive role in directing GLR-1 retrograde transport, we generated P_{glr-1}::*rab-6.2(gtp)*, a transgene that expresses GTPase-defective, constitutively active RAB-6.2 via the *glr-1* promoter. Expression of RAB-6.2(GTP) resulted in the accumulation of few GLR-1::GFP ventral cord puncta and, instead, resulted in the accumulation in several large puncta in the neuron cell bodies (Fig. 6, A–D, I, and J). We examined GLR-1::GFP in animals that express RAB-6.2(GTP) and are also blocked for endocytosis. We found that both the decrease in GLR-1 ventral cord puncta and the accumulation of GLR-1 in large cell body puncta caused by RAB-6.2(GTP) are prevented in *unc-11* mutants (Fig. 6, E–J). Similarly, GLR(4KR)::GFP puncta levels remain steady in the dendrites of animals expressing RAB-6.2(GTP) (Fig. 6 J; and Fig. S1 A). Moreover, coexpression of dominant-negative VPS-4 does not suppress the decrease in dendritic GLR-1 or the accumulation of GLR-1 in the cell body in animals expressing RAB-6.2(GTP) (Fig. S1 A and not depicted). Thus, RAB-6.2(GTP) promotes the retrograde redistribution rather than the turnover of previously endocytosed GLR-1 receptors.

If RAB-6.2(GTP) is driving GLR-1 out of synapses, we would expect a reduction in GLR-1 function. We therefore
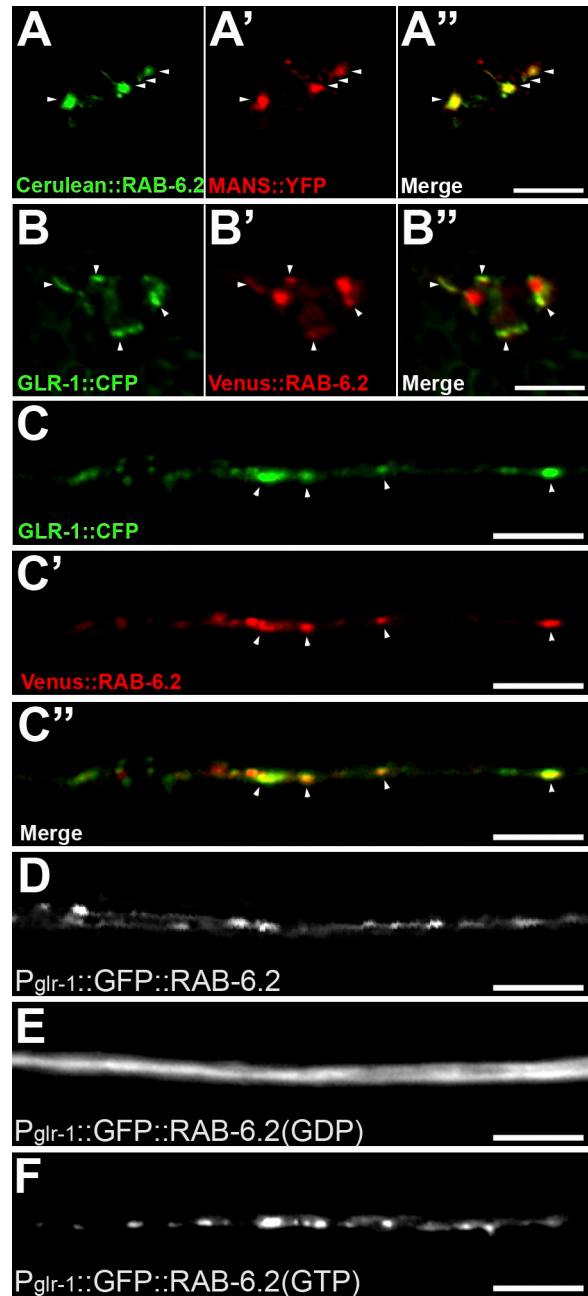

Figure 5. **RAB-6.2 associates with Golgi and GLR-1.** (A and A') Cerulean::RAB-6.2 (A) and MANS::YFP (A') in PVC cell bodies. (A'') Merged image showing Cerulean::RAB-6.2 colocalization to puncta with MANS::YFP (arrowheads). (B–C'') GLR-1::CFP (B and C) and Venus::RAB-6.2 (B' and C') in PVC cell bodies (B–B'') and dendrites (C–C''). (B'' and C'') Merged images show colocalization at specific points (arrowheads). (D–F) Subcellular localization of the indicated GFP::RAB-6.2 variant: wild type (D), GDP-locked mutant (E), and GTP-locked mutant (F). Bars, 5 µm.

measured the spontaneous reversal rate and mechanosensitivity of animals expressing *RAB-6.2(GTP)* and found that both behaviors were reduced (Fig. 6 K and not depicted). To determine the site of GLR-1 accumulation in the cell body, we expressed RAB-6.2(GTP) in *odIs25[P_{glr-1}::glr-1::cfp]* transgenic animals that also express MANS::YFP, which resides in the Golgi (Rolls et al., 2002; Shim et al., 2004). In wild-type cell bodies, little GLR-1::CFP is colocalized with MANS::YFP (Fig. 6 L).
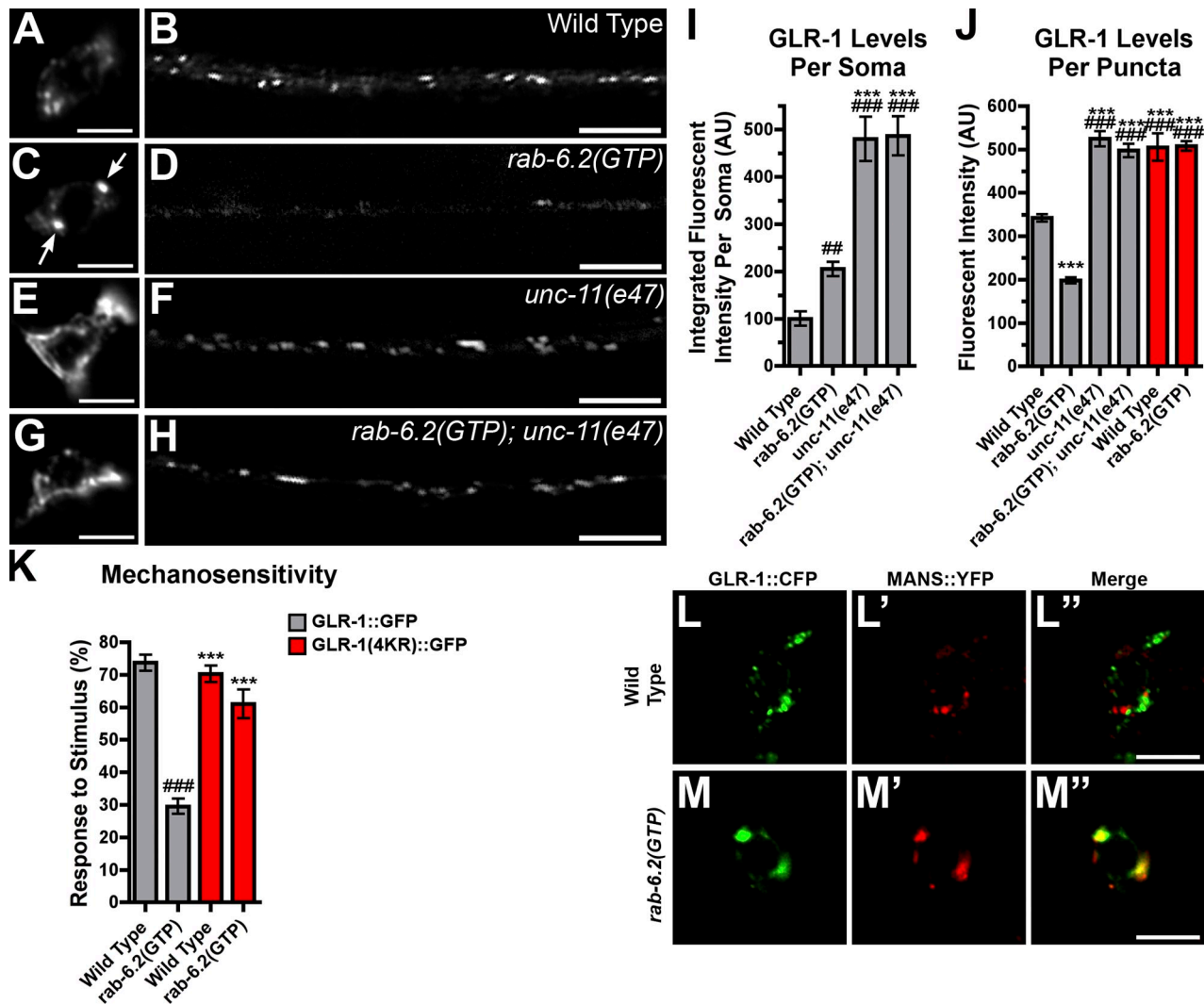
Figure 6. **RAB-6.2 drives GLR-1::GFP into Golgi.** (A–H) GLR-1::GFP in wild type (A and B), *rab-6.2(GTP)*–expressing transgenic animals (C and D), *unc-11(e47)* mutants (E and F), and *rab-6.2(GTP); unc-11(e47)* double mutants (G and H). Arrows indicate punctate GLR-1 accumulation in the cell body. (I–K) The mean integrated fluorescent intensity for individual PVC cell bodies (I), fluorescent intensity of GLR-1 fluorescent puncta (J), and nose-touch mechanosensitivity (K). (L–M″) GLR-1::CFP (L and M) and MANS::YFP (L′ and M′) fluorescence in cell bodies (PVC shown) for wild-type animals (L–L″) and animals expressing *rab-6.2(GTP)* (M–M″). Bars, 5 µm. ANOVA with Dunnett's multiple comparison to wild type (##, P < 0.01; ###, P < 0.001) or *rab-6.2(GTP)* mutants expressing GLR-1::GFP (***, P < 0.001). Error bars are SEM. AU, arbitrary unit.

In contrast, expression of RAB-6.2(GTP) drives GLR-1::CFP into MANS::YFP-decorated Golgi (Fig. 6 M).

Activated RAB-6.2 interacts with LIN-10

One possible effector target of RAB-6.2 could be LIN-10, a PDZ/phosphotyrosine binding (PTB) scaffolding molecule that regulates GLR-1 recycling (Glodowski et al., 2007; Park et al., 2009). The PTB domain of Mint3, a mammalian LIN-10 homologue, can directly bind to mammalian Rab6 (Teber et al., 2005; Thyrock et al., 2010). We therefore tested whether LIN-10 PTB domain bait and various *C. elegans* candidate Rab prey could interact by yeast two-hybrid assay. We tested 19 different Rab preys and found an interaction for RAB-6.1 and RAB-6.2, members of the Rab6 subfamily (Fig. S3).

To confirm the physical interaction between the LIN-10 PTB domain and RAB-6.2, we expressed either GST or GST::LIN-10(PTB), which contains GST plus 207 amino acids

containing the LIN-10 PTB domain in bacteria and then tested the ability of these proteins when bound to glutathione agarose beads to pull down in vitro translated HA-tagged RAB-6.2 protein. We also tested the ability of GST::LIN-10(PTB) to interact with mutant RAB-6.2 protein locked in either its GTP-bound or GDP-bound state. GST alone could not pull down HA::RAB-6.2 protein (Fig. 7 A). However, GST::LIN-10(PTB) could specifically pull down HA::RAB-6.2(GTP) but not HA::RAB-6.2(GDP) (Fig. 7 A). We also expressed either GST alone, GST::RAB-6.2(GDP), or GST::RAB-6.2(GTP) in bacteria and then tested the ability of these proteins to pull down an in vitro translated HA-tagged LIN-10 PTB domain. We found that GST::RAB-6(GTP), but not GST or GST::RAB-6(GDP), specifically pulled down HA::LIN-10(PTB) (Fig. 7 B). Thus, activated RAB-6.2 can physically bind to LIN-10.

We next introduced the $P_{glr-1}::venus::rab-6.2$ transgene into animals that express a LIN-10::CFP chimeric protein to
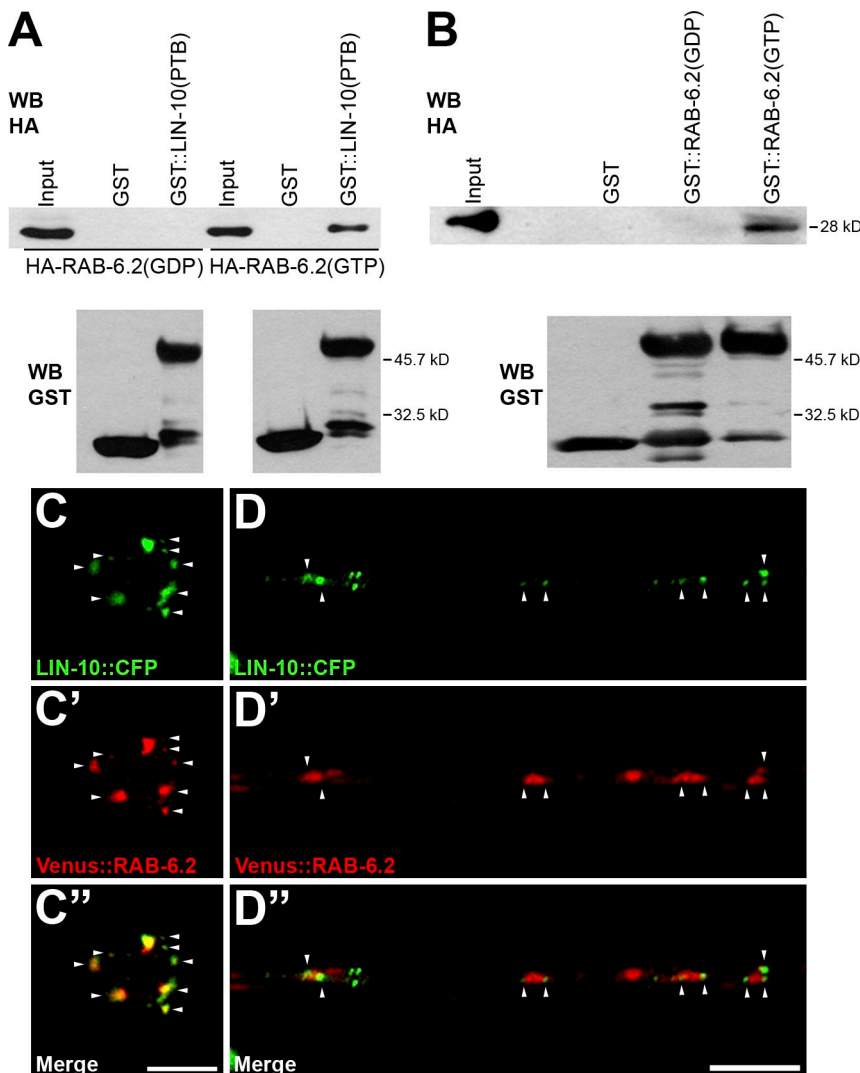
Figure 7. **RAB-6.2 binds to and is colocalized with LIN-10.** (A) Pull-down experiments using GST:: LIN-10(PTB) or GST alone incubated with in vitro translated fusion proteins HA::RAB-6.2(GDP) or HA::RAB-6.2(GTP). (B) Pull-downs using GST::RAB-6.2(GDP), GST::RAB-6.2(GTP), or GST alone incubated with in vitro translated fusion protein HA:: LIN-10(PTB). 10% of input was loaded as a control. (C–D') LIN-10::CFP (C and D) and Venus::RAB-6.2 (C' and D') in neurons. (C'' and D'') Colocalization of LIN-10::CFP and Venus::RAB-6.2 was detected in both PVC cell bodies (C'', arrowheads) and ventral cord dendrites (D'', arrowheads). Bars, 5 µm. WB, Western blot.

determine where in neurons this physical interaction occurs. LIN-10 is localized to Golgi structures in neuron cell bodies and punctate structures along ventral cord dendrites (Glodowski et al., 2005). We found that Venus::RAB-6.2 is colocalized with LIN-10::CFP in neuron cell bodies (Fig. 7 C). Along dendrites, Venus::RAB-6.2 is colocalized adjacent to sites of LIN-10 localization (Fig. 7 D), indicating that these two proteins are found at related subcellular compartments within neurons.
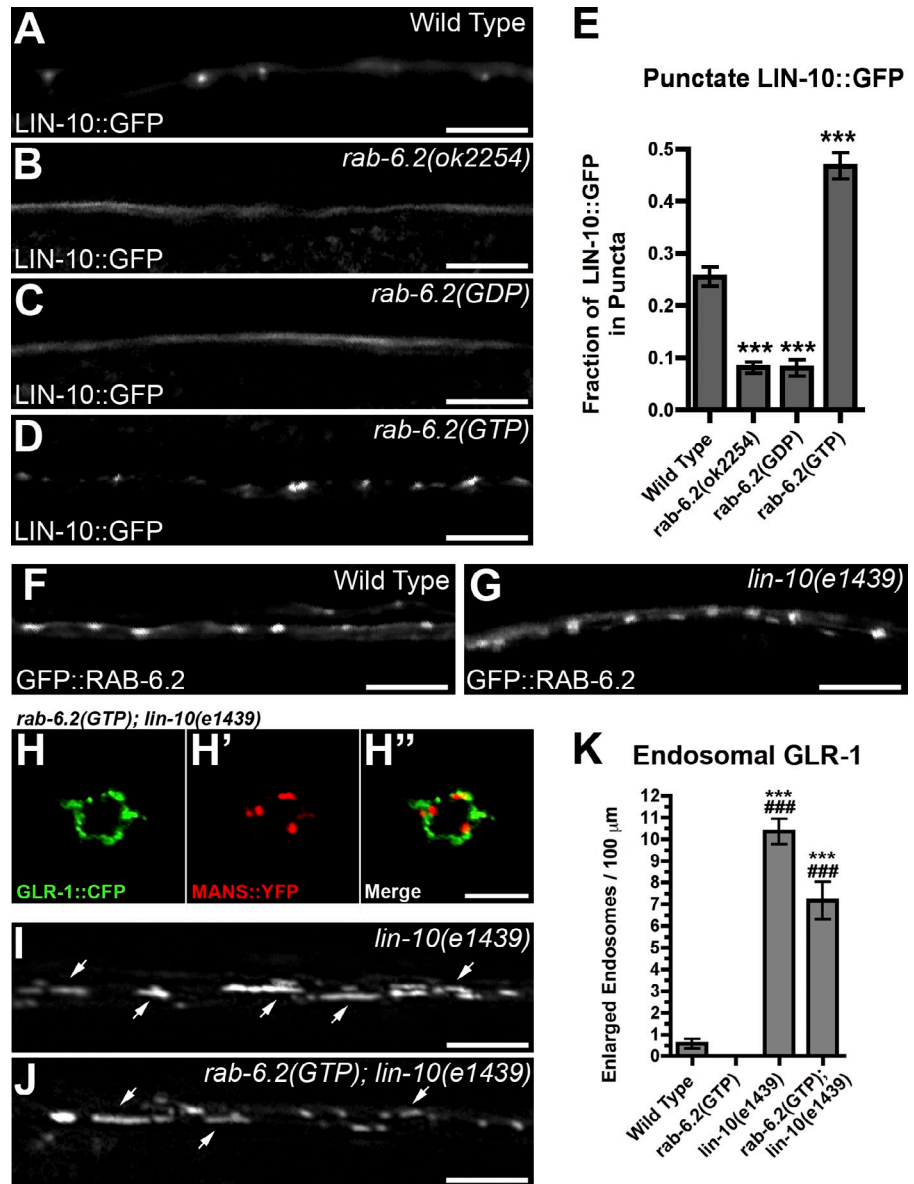
Both LIN-10 and RAB-6.2 are broadly expressed in multiple tissues, including the intestine (Fig. 2; Whitfield et al., 1999). *C. elegans* intestinal cells are polarized epithelial cells that are well suited for subcellular trafficking experiments (Grant and Sato, 2006). To examine LIN-10 and RAB-6.2 in epithelial cells, we generated transgenes containing the *vha-6* intestine-specific promoter sequences driving sequences encoding GFP, tagRFP, or mCherry fused in frame to the complete RAB-6.2, MANS, or LIN-10 reading frame sequences. Both LIN-10::GFP and tagRFP::RAB-6.2 proteins were localized to punctate structures in the intestinal cytosol (Fig. S4 A). Similarly, both GFP::RAB-6.2 and MANS::mCherry were completely colocalized (Fig. S4 B). Finally, we found that LIN-10::GFP and MANS::mCherry were localized adjacent

to one another in the intestine (Fig. S4 C). Collectively, our results suggest that RAB-6.2 is localized tightly to MANS-containing Golgi structures and that LIN-10 is localized to adjacent Golgi-associated structures.

LIN-10 is an effector of RAB-6.2

To test whether LIN-10 is a RAB-6.2 effector, we first examined whether RAB-6.2 acted to recruit LIN-10 by introducing the *odIs22[P_{glr-1}::lin-10::GFP]* transgene into *rab-6.2* mutants. Although LIN-10::GFP is punctate in wild type (Fig. 8 A), it is diffusely distributed in the cytosol of *rab-6.2* mutants (Fig. 8 B). We next introduced transgenes expressing either RAB-6.2(GDP) or RAB-6.2(GTP) into *odIs22* animals. Like in *rab-6.2* mutants, LIN-10::GFP is not localized to puncta when RAB-6.2(GDP) is expressed (Fig. 8 C). In contrast, expression of RAB-6.2(GTP) drove LIN-10::GFP into a more punctate localization pattern (Fig. 8 D), suggesting that the activation of RAB-6.2 regulates LIN-10 subcellular localization. Using fluorescence density thresholding (Umemura et al., 2005), we were able to approximate the relative levels of LIN-10::GFP present in puncta versus the unlocalized baseline along the ventral cord (Fig. 8 E). We observed no difference

Figure 8. **RAB-6.2 regulates LIN-10 localization.** (A–D) LIN-10::GFP in wild-type (A), *rab-6.2(ok2254)* (B), *rab-6.2(GDP)*–expressing (C), and *rab-6.2(GTP)*–expressing (D) animals. (E) Fraction of ventral cord LIN-10::GFP fluorescence concentrated into puncta relative to the total. (F and G) GFP::RAB-6.2 in wild-type animals (F) and *lin-10(e1439)* mutants (G). (H and H') GLR-1::CFP (H) and MANS::YFP (H') in interneuron cell bodies. (H'') Colocalization was examined in the merged image for *rab-6.2(GTP); lin-10(e1439)* double mutants. (I–K) GLR-1::GFP in *lin-10(e1439)* mutants (I) and *rab-6.2(GTP); lin-10(e1439)* double mutants (J). GLR-1 accumulates in enlarged endosomes (arrows), quantified in K. Bars, 5 μm. ANOVA with Dunnett's multiple comparison to wild type (***, P < 0.001) or *rab-6.2(GTP)* (###, P < 0.001). Error bars are SEM.

in GFP::RAB-6.2 puncta in wild type (Fig. 8 F) compared with *lin-10* mutants (Fig. 8 G), indicating that whereas RAB-6.2 regulates LIN-10 subcellular localization, the reverse is not true.

If LIN-10 is a RAB-6.2 effector, the effect of RAB-6.2 on GLR-1 retrograde transport should require LIN-10 activity. Although RAB-6.2(GTP) can drive GLR-1::CFP to colocalize with MANS::YFP in wild type (Fig. 6 M), it cannot in *lin-10* mutants (Fig. 8 H). We also examined GLR-1::GFP ventral cord localization in transgenic animals expressing RAB-6.2(GTP), which are also mutated for *lin-10*. In *lin-10* mutants, GLR-1 accumulates in elongated postendocytic endosomes that are readily distinguished based on their size and morphology (Glodowski et al., 2007; Park et al., 2009). We found that if LIN-10 activity is absent, GLR-1::GFP accumulates in elongated endosomes along ventral cord dendrites regardless of the presence of RAB-6.2(GTP) (Fig. 8, I–K). Thus, RAB-6.2 promotes the retrograde transport of GLR-1 receptors back to Golgi at least in part through its interaction with LIN-10 as an effector. As GLR-1 receptors accumulate in elongated endosomes in *lin-10* mutants, we speculate that LIN-10 also plays a separate, RAB-6.2–independent role in transporting GLR-1 from early endosomes to the degradation pathway.

The retromer regulates GLR-1 recycling

Another mediator of retrograde transport is the retromer complex. Thus, we examined GLR-1::GFP localization in the retromer mutants *snx-1(tm847)* and *vps-35(hu68)* as well as mutants for the SNX-1–associated *rme-8(b1023)*. We found a significant decrease in the number and fluorescent intensity of GLR-1::GFP puncta in all three of these mutants (Fig. 9, A–D, and G; and Fig. S1 A) similar to the phenotype observed in *rab-6.2* mutants, suggesting that the retromer also promotes GLR-1 recycling. Mutations that impaired GLR-1 endocytosis or ubiquitination blocked the effects of these retromer mutants (Fig. 9 G, Fig. S1, and not depicted), indicating that the retromer regulates GLR-1 trafficking at a step after endocytosis. Finally, turnover
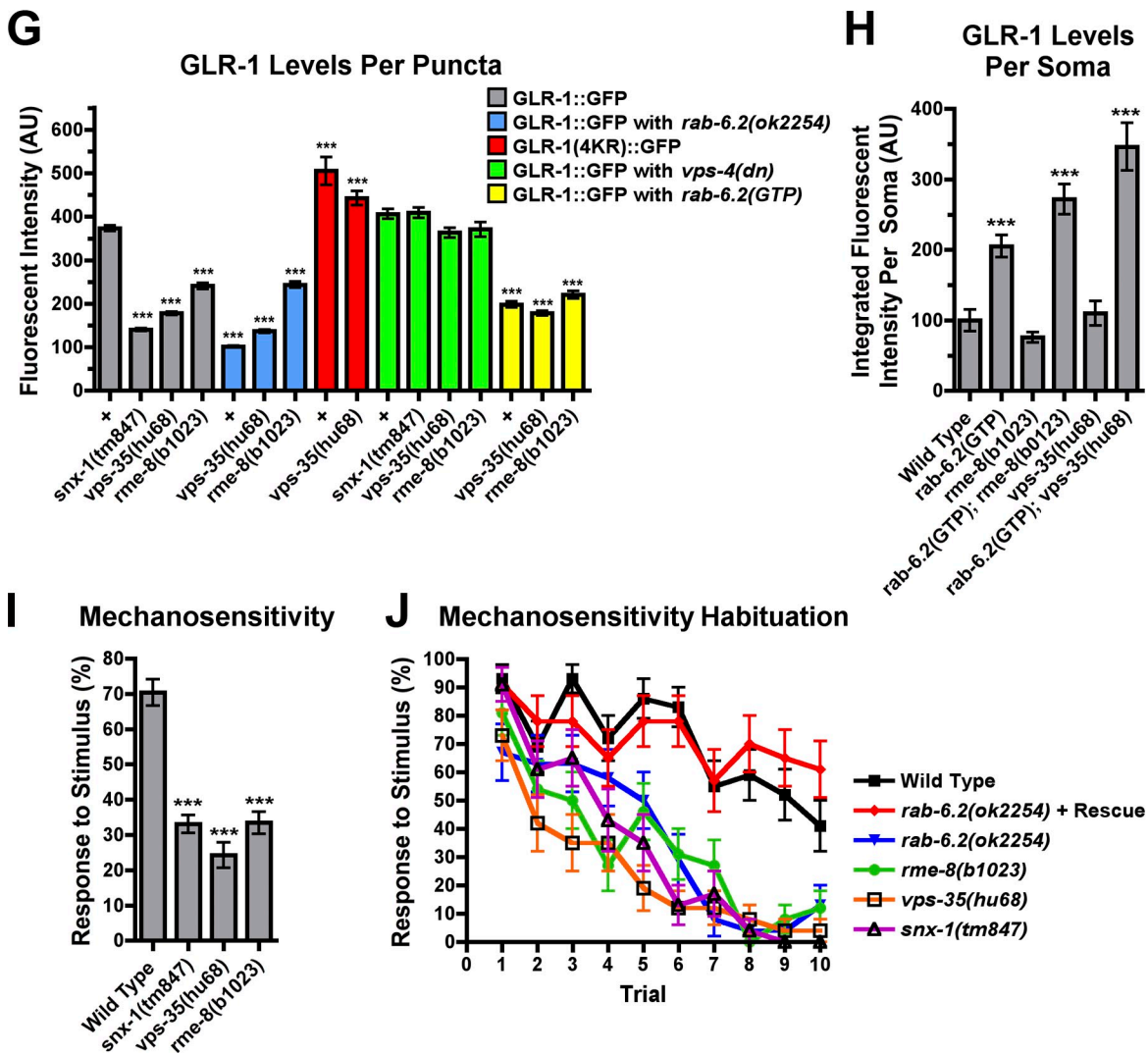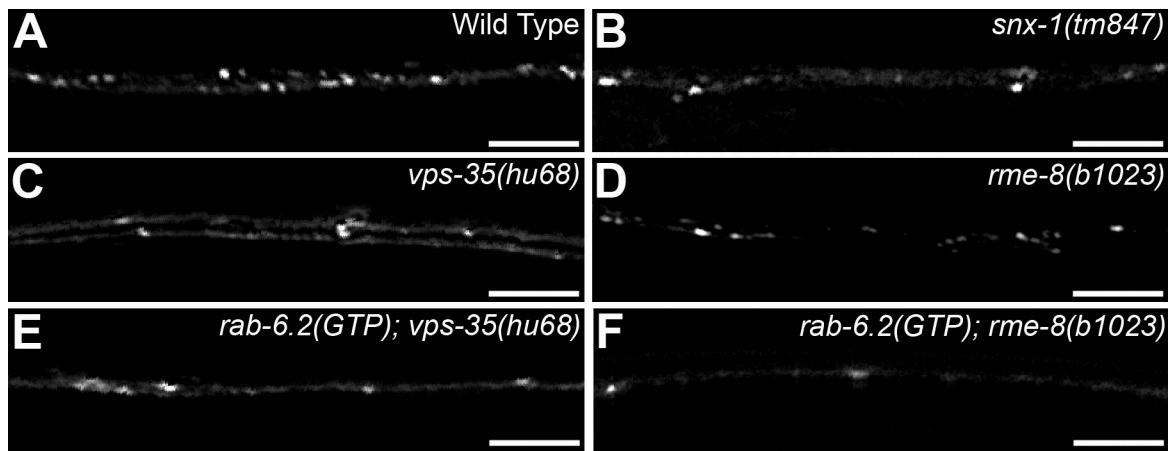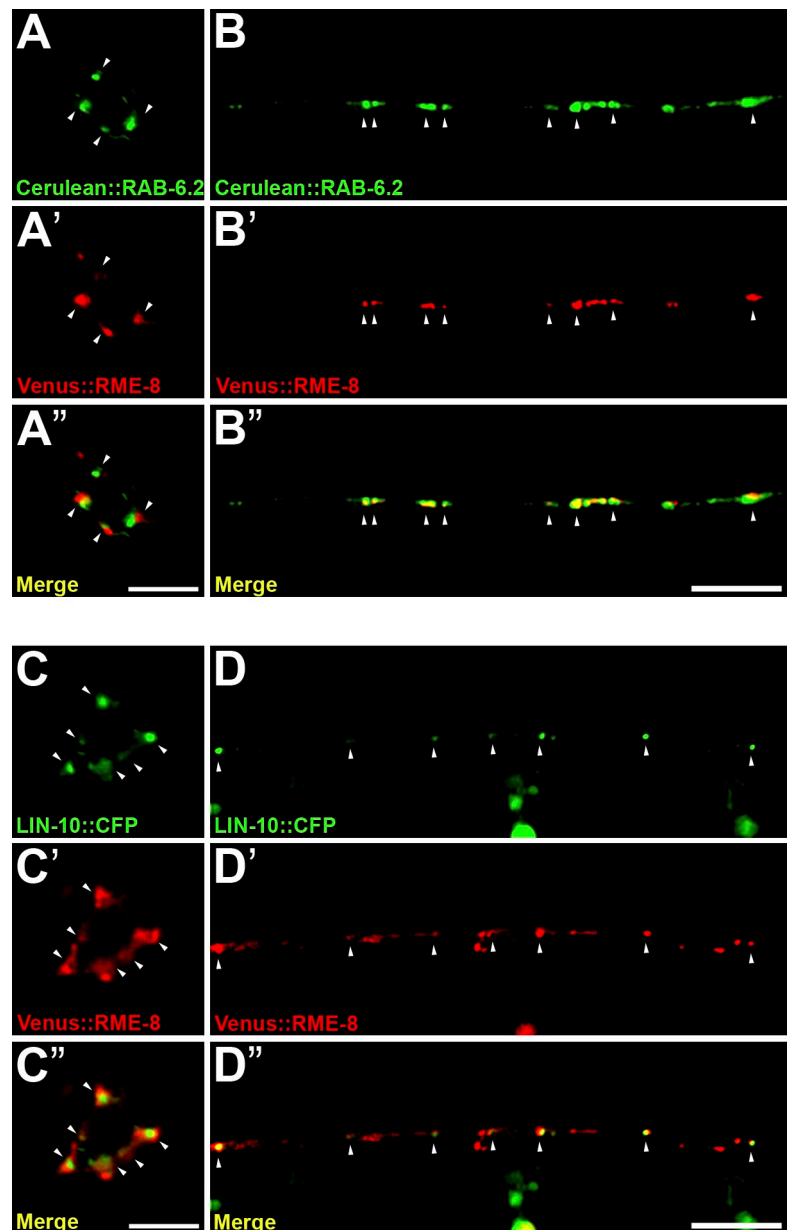
Figure 9. **The retromer regulates GLR-1 retrograde transport.** (A–F) GLR-1::GFP in wild type (A), *snx-1(tm847)* (B), *vps-35(hu68)* (C), *rme-8(b1023)* (D), *rab-6.2(GTP)*–expressing *vps-35(hu68)* (E), and *rab-6.2(GTP)*–expressing *rme-8(b1023)* (F) animals. (G) Mean fluorescent intensity of GLR-1 puncta (plus sign indicating wild type). (H and I) The mean integrated fluorescent intensity for individual PVC cell bodies (H) and nose-touch mechanosensitivity (I). (J) Mean nose-touch mechanosensory response is plotted for each trial during a train of nose-touch trials over a 5-min period. Genotypes are indicated by color. Rescue indicates *rab-6.2(ok2254)* mutants that express wild-type Venus::RAB-6.2 from the *glr-1* promoter. Bars, 5 µm. ANOVA with Dunnett's multiple comparison to wild type (***, P < 0.001). Error bars are SEM. AU, arbitrary unit.

Figure 10. RAB-6.2 and LIN-10 colocalize with RME-8 in neurons. (A–D) Fluorescence from neuron cell bodies (A and C) and ventral cord dendrites (B and D) is shown. (A–B'') Cerulean::RAB-6.2 (A and B) colocalizes with Venus::RME-8 (A' and B'; A'' and B'' show merged). (C–D'') LIN-10::CFP (C and D) colocalizes with Venus::RME-8 (C' and D'; C'' and D'' show merged). Arrowheads indicate colabeled puncta. Bars, 5 µm.

of GLR-1 in these retromer mutants is blocked when dominant-negative VPS-4 is expressed, suggesting that, in the absence of retromer function, GLR-1 is shunted by the ESCRT complex to MVBs, late endosomes, and lysosomes for proteolysis (Fig. 9 G and Fig. S1 A).

To examine whether RAB-6.2 and the retromer regulate GLR-1 via the same pathway, we performed an epistasis analysis between *rab-6.2* and the retromer mutations. Double mutants for *rab-6.2* and either *rme-8* or *vps-35* did not show a dramatically stronger effect on GLR-1 cluster number, suggesting either that these genes function in the same genetic pathway or that the retrograde pathway is completely blocked in the absence of either RAB-6.2 or the retromer alone, occluding a stronger phenotype in the double mutant (Fig. 9 G and Fig. S1 A). We also generated double mutants that contain a GTP-locked $P_{glr-1}::rab-6.2(gtp)$ transgene, which can drive GLR-1::GFP retrograde transport from dendrites back to the cell body, and

either a *vps-35* (Fig. 9 E) or *rme-8* (Fig. 9 F) mutation. We found that RAB-6.2(GTP) can drive GLR-1::GFP retrograde transport back to the cell body regardless of the presence of VPS-35 or RME-8 activity (Fig. 9 H), suggesting that RAB-6.2 and the retromer complex can independently mediate GLR-1 retrograde transport under certain circumstances.

If RAB-6.2 and the retromer both promote GLR-1 retrograde recycling, we would expect RAB-6.2 and retromer components to be localized either together or nearby. The J domain protein RME-8 associates with the retromer complex, where it helps regulate clathrin dynamics at early endosomes (Shi et al., 2009). Thus, we coexpressed Cerulean::RAB-6.2 with Venus::RME-8 in the command interneurons, and we observed that the two proteins were localized to either the same or adjacent puncta in both the neuron cell body (Fig. 10 A) or the dendrites (Fig. 10 B). We also found that LIN-10::CFP and Venus::RME-8 were colocalized (Fig. 10, C and D), often with Venus::RME-8

fluorescence surrounding LIN-10::CFP puncta. We also used the intestinal *vha-6* promoter to coexpress either GFP::RAB-6.2 (Fig. S4 D) or LIN-10::GFP (Fig. S4 E) with mCherry::RME-8. GFP::RAB-6.2 was localized to puncta adjacent to mCherry::RME-8–labeled puncta, whereas LIN-10::GFP and mCherry::RME-8 showed an identical colocalization pattern in the intestine. Our results suggest that RAB-6.2, LIN-10, and the retromer complex are localized along an endosome–Golgi axis, where they together promote the retrograde recycling of cargo molecules, such as GLR-1.

The observed decrease in GLR-1–containing AMPARs along retromer mutant dendrites should also result in depressed GLR-1–mediated behaviors. Indeed, we found that retromer mutants have a similar low level of mechanosensitivity as *rab-6.2* mutants (Fig. 9 I). Mechanosensitivity is assayed by presenting a train of physical stimuli to the tip of the animal's nose over a 5-min period, determining whether the animal responds by immediately reversing direction after each stimulus, and then averaging all of the stimuli from 10 consecutive trials for a given animal. Whereas nearly all wild-type animals respond to the first stimulus, only about half respond by trial 10, suggesting a slow rate of habituation. In contrast, *rab-6.2* mutants and retromer mutants also respond robustly to the first stimulus but rapidly habituate to a response rate of <10% by trial 7 (Fig. 9 J). The rapid habituation observed in *rab-6.2* mutants is fully rescued by the expression of a rescuing wild-type Venus::RAB-6.2 from the *glr-1* promoter, suggesting that RAB-6.2 and retrograde transport of AMPARs not only maintain glutamatergic efficacy but also regulate the habituation kinetics of the touch circuit in the postsynaptic interneurons.

Discussion

Here, we have shown that RAB-6.2 and LIN-10 recycle AMPARs along a retrograde transport pathway in neurons so as to maintain synaptic strength (Fig. S5). GLR-1 AMPARs undergo activity-dependent endocytosis in a process that requires UNC-11/AP180 (Fig. S5 A; Burbea et al., 2002; Grunwald et al., 2004; Glodowski et al., 2007). Once endocytosed, AMPARs can either be sent to MVBs for eventual degradation, or they can be recycled back to the synapse. We propose that RAB-6.2 performs two functions to promote the recycling fate for these receptors. First, RAB-6.2, in its GTP-bound form, interacts with LIN-10, delivering LIN-10 to early endosomes (Fig. S5 B). We suggest that LIN-10, along with the retromer complex and RME-8, sequesters AMPARs into endosomal tubules that in turn give rise to retrograde cargo vesicles for the receptors (Fig. S5 C). Second, RAB-6.2, in its GTP-bound form, regulates the trafficking of these cargo vesicles to Golgi, including dendritic outpost Golgi as well as cell body Golgi (Fig. S5 D). Interestingly, RAB-6.2–decorated Golgi and LIN-10/RME-8–decorated endosomes are adjacent to one another in neurons and epithelia cells, perhaps indicating that Golgi-proximal endosomes favor this pathway. Once at Golgi, AMPARs can affiliate with new coreceptors and be resorted back to synaptic membranes (Fig. S5 E). Our results suggest that GLR-2–containing AMPARs do not rely on this pathway, indicating that different trafficking

pathways, such as the retrograde pathway, are used for subunit-specific AMPAR regulation.

Why would a channel use the retrograde pathway? Interestingly, several transporters have recently been shown to be retrograde cargo. The auxin efflux transporter PIN1 uses the retrograde pathway to move from the basal pole to the lateral face of stele cells (Jaillais et al., 2006, 2007). The Menkes protein copper transporter and the reductive iron transporter Fet3–Ftr1 are redistributed in the cell by the retrograde pathway in response to changes in copper and iron concentration (Petris and Mercer, 1999; Strochlic et al., 2007). Finally, the GLUT4 glucose transporter, which is regulated by insulin, uses the retrograde pathway to return to Golgi for repackaging into new storage vesicles (Shewan et al., 2003). Recently, *N*-methyl-D-aspartic acid receptors have been observed to traffic to Golgi outposts via an unknown pathway that utilizes SAP97 and calcium/calmodulin-dependent serine protein kinase (Jeyifous et al., 2009). Our findings raise the possibility that mammalian *N*-methyl-D-aspartic acid receptors and GLR-1 share an evolutionarily conserved transport pathway or that trafficking of multiple glutamate receptor types through Golgi outposts is mediated by the retrograde transport pathway.

Signaling molecules, such as Wntless/MIG-14, also use the retrograde pathway. Wntless is a sorting receptor for the Wnt family of morphogens, shepherding them along the secretory pathway for eventual secretion (Pan et al., 2008; Yang et al., 2008; Shi et al., 2009). Retrograde transport of Wntless/MIG-14 allows it to return to the Golgi to associate with a nascent Wnt cargo molecule for another round of secretion. Like Wnt, AMPAR channels require a complex set of chaperones and coreceptors for surface delivery, and AMPAR channels themselves exist in diverse combinations of subunits, each with different trafficking fates and channel gating properties (Payne, 2008; Díaz, 2010; Henley et al., 2011). Thus, retrograde transport might allow the channel to associate with new or different chaperones or coreceptors. In support of this idea, we observed that although GLR-1 localization is impaired when retrograde transport was blocked, the localization of STG-1 (Wang et al., 2008) and SOL-1 (Zheng et al., 2004) seems unaffected. This would suggest that coreceptor interactions are reversible in vivo, with channels and coreceptors coming apart and reassembling according to the particular trafficking pathway being used. Recently, the Cornichon homology protein CNIH-2 has been shown to associate with AMPARs, although its exact role is controversial (Schwenk et al., 2009; Brockie and Maricq, 2010; Kato et al., 2010; Shi et al., 2010). We found a single CNIH-2 homologue in the *C. elegans* genome and showed that it is localized to puncta along dendrites in a manner that also requires retrograde transport.

Different combinations of AMPAR subunits themselves undergo different trafficking fates (Henley et al., 2011). AMPARs with "long tail" subunits (e.g., GluA1) are delivered into synapses in response to activity, whereas AMPARs with "short tail" subunits (e.g., GluA2) tend to cycle continuously in and out of synapses (Chung et al., 2000; Hayashi et al., 2000; Passafaro et al., 2001; Shi et al., 2001; Esteban et al., 2003; Lu and Ziff, 2005). We found that RAB-6.2 regulates

GLR-1–containing channels but not GLR-2–containing channels; thus, GLR-1 homomeric channels and GLR-1/GLR-2 heteromeric channels might use different pathways for their recycling. Interestingly, these subunits have different affinities for scaffolding molecules, show different trafficking patterns in response to previous mechanosensory experience, and yield different habituation kinetics within the touch circuit (Emtage et al., 2009). Thus, RAB-6.2–mediated trafficking might play an important role in this or other types of behavioral plasticity in the touch circuit by dictating the specific GLR-1/GLR-2 subunit composition at the synapse. Indeed, animals displayed faster habituation to touch in mutants defective for the retrograde transport of GLR-1–containing AMPARs. Future tests of this idea will require a more thorough means for discriminating the subunit combinations.

The role of retrograde transport in neurons is poorly understood with one important exception: the amyloid precursor protein (APP). Changes in retromer gene expression are correlated with Alzheimer's disease (AD), and depletion of the retromer increases the production of Aβ, one of the key pathological causes of AD (Small, 2008). Neuronal SorLA (sorting protein-related receptor) associates with APP and helps regulate APP retrograde transport to the Golgi; SorLA is also reduced in AD brains (Scherzer et al., 2004; Andersen et al., 2005; Offe et al., 2006; Nielsen et al., 2007). Retrograde transport also appears to help recycle the β-secretases BACE1 and BACE2, which influence Aβ production (He et al., 2005; Wahle et al., 2005). Thus, APP retrograde transport might keep Aβ production low in healthy neurons by keeping APP out of the endosome, the site where it becomes processed to produce Aβ. Consistent with this idea, the Mints, which are orthologues of LIN-10, regulate APP and presenilin trafficking, as well as APP processing into Aβ, although the exact mechanism remains controversial (Sastre et al., 1998; Mueller et al., 2000; Hill et al., 2003; Lee et al., 2003; Xie et al., 2005; Sano et al., 2006; Ho et al., 2008; Saito et al., 2008). Our results indicate that Mint proteins are effectors for Rab6 GTPases in neurons and could help explain how an evolutionarily conserved choice point in trafficking regulated by Mint-Rab6 has been co-opted for a pathological function in human disease.

Materials and methods

Strains
Animals were grown at 20°C on standard nematode growth media (NGM) plates seeded with OP50 *Escherichia coli*. Some strains were provided by the *Caenorhabditis* Genetics Center. Strains were backcrossed to our laboratory N2 strain to minimize other genetic variation. The following strains were used: *glr-1(ky176)*, *lin-10(e1439)*, *nuIs108[P_glr-1::glr-1(4kr)::gfp]*, *nuIs145[P_glr-1::vps-4(dn)]* (a gift from J. Kaplan, Massachusetts General Hospital, Boston, MA), *nuIs25[P_glr-1::glr-1::gfp]*, *P_glr-1::mans::yfp]*, *odEx[P_glr-1::cerulean::rab-6.2(+)]*, *P_glr-1::mans::yfp]*, *odEx[P_glr-1::cerulean::rab-6.2(+)]*, *odEx[P_glr-1::gfp::cnih-2]*, *odEx[P_glr-1::gfp::rab-6.2(+)]*, *odEx[P_glr-1::gfp::rab-6.2(gdp)]*, *odEx[P_glr-1::gfp::rab-6.2(gtp)]*, *odEx[P_glr-1::lin-10::cfp, P_glr-1::venus::rme-8]*, *odEx[P_glr-1::mans::yfp]*, *odEx[P_glr-1::mans::yfp]*, *odEx[P_glr-1::mrfp::syntaxin-13]*, *odEx[P_glr-1::rab-6.2(+)]*, *odEx[P_glr-1::rab-6.2(gtp)]*, *odEx[P_glr-1::sol-1::gfp]*, *odEx[P_glr-1::stg-1::gfp]*, *odEx[P_glr-1::venus::rab-6.2(+), P_glr-1::lin-10::cfp]*, *odEx[P_glr-1::venus::rab-6.2(+)]*, *odEx[P_glr-2::gfp::glr-2]*, *odEx[P_rab-6.2::gfp]*, *odEx[P_vha-6::gfp::rab-6.2(+)]*, *odEx[P_vha-6::mans::mcherry]*, *odEx[P_vha-6::tagrfp::rab-6.2(+)]*, *odIs1[P_glr-1::snb-1::gfp]*, *odIs22[P_glr-1::lin-10::gfp]*,

odIs25[P_glr-1::glr-1::cfp], *odIs6[P_glr-1::mrfp]*, *pwIs[P_vha-6::lin-10::gfp]*, *pwIs[P_vha-6::mcherry::rme-8]*, *pwIs[P_vha-6::venus::rme-8]*, *rab-6.2(ok2254)* (a gift from S. Mitani, Tokyo Women's Medical University, Tokyo, Japan), *rhIs4[P_glr-1::gfp]* (a gift from W. Wadsworth, University of Medicine and Dentistry of New Jersey, Piscataway, NJ), *rme-8(b1023)*, *snx-1(tm847)*, *unc-11(e47)*, and *vps-35(hu68)*.

Transgenes and germline transformation
Transgenic strains generated in this study were isolated after microinjecting various plasmids (5–50 ng/ml) using *rol-6dm* (a gift from C. Mello, University of Massachusetts Medical School, Worcester, MA), *ttx-3::rfp* and *ttx-3::gfp* (a gift from O. Hobert, Columbia University, New York, NY), or *lin-15(+)* (a gift from J. Mendel, California Institute of Technology, Pasadena, CA) as a marker. Plasmids containing the *glr-1* (a gift from V. Maricq, University of Utah, Salt Lake City, UT) or *vha-6* promoters followed by the indicated cDNA construct were generated using standard techniques. Plasmids for examining *rab-6.2* gene expression were made by PCR of 2 kb of upstream promoter sequence as well as complete coding sequences and introns and then subcloning the resulting product into a GFP expression vector. Transgenic animals expressing GFP::GLR-2 were generated by injecting pPB66 (Mellem et al., 2002). All resulting transgenes were introduced into the germline and followed as extrachromosomal arrays. The fluorophore-tagged reporters described in this paper have been previously demonstrated to be functional, except for RAB-5, RAB-7, and MANS, as mutants for their corresponding genes either do not exist or are lethal and thus cannot be easily tested for functionality.

Fluorescence microscopy
GFP- and RFP-tagged fluorescent proteins were visualized in nematodes by mounting young adult animals on 2% agarose pads with levamisole. Fluorescent images were observed using a microscope (Axioplan II; Carl Zeiss). A 100×, NA 1.4 Plan Apochromat oil immersion objective was used to detect GFP, Venus, CFP, Cerulean, mCherry, and mRFP signals of worms mounted on 2% agarose pads at room temperature. Imaging was performed with a charge-coupled device camera (ORCA-ERG 1394; Hamamatsu Photonics) using iVision v4.0.11 (BioVision Technologies) software. Exposure times were chosen to fill the 12-bit dynamic range without saturation. Maximum intensity projections of z-series stacks were obtained, and out of focus light was removed with a constrained iterative deconvolution algorithm (iVision). For most images, we captured the ventral cord dendrites in the retrovesicular ganglion region surrounding the RIG and AVG cell bodies.

The quantification of ventral nerve cord fluorescent objects (i.e., puncta and enlarged endosomes) was performed using ImageJ (National Institutes of Health) to automatically threshold the images and then determine the outlines of fluorescent objects in ventral cord dendrites. ImageJ was used to quantify both the shape and the size of all individual fluorescent objects along the ventral cord. This allowed us to distinguish between the small GLR-1::GFP puncta in wild-type animals and the enlarged aberrant endosomes (which have an elongated shape not observed in wild type) in mutants. Object size was measured as the maximum diameter for each outlined cluster. Object number was calculated by counting the mean number of clusters per 100 µm of dendrite length.

The quantification of PVC cell body fluorescence was performed using ImageJ to measure the integrated fluorescent density (the sum of all detectable pixel intensities per cell body) for each neuron. For the quantification of GLR-1::GFP and mRFP::SYN-13 colocalization, we fixed animals with ice-cold 1% paraformaldehyde in PBS for 10 min and imaged them using a previously published protocol (Chun et al., 2008; Park et al., 2009). Images for neuronal cell bodies were taken using a confocal microscope equipped with the confocal imager (CARV II; BD) and a 100× Plan Apochromat objective, NA 1.4 (Carl Zeiss).

For quantitative colocalization analysis, all image manipulations were performed with iVision (v4.0.11) software using the fluorescent color voxels colocalization function. We applied an empirically derived threshold to all images for both the GLR-1::GFP channel and the mRFP::SYN-13 channel to eliminate background coverslip fluorescence and other noise (typically, <5% of pixels for each channel). The fluorescent intensity values for both the GLR-1::GFP and mRFP::SYN-13 channels were then scatter plotted for each pixel. Pixels with similar intensity values for both channels (within an empirically established tolerance factor) were counted as colocalized. To acquire the fraction of GLR-1::GFP colocalized with mRFP::SYN-13, the number of colocalized pixels was normalized to the number of GLR-1::GFP pixels under threshold. To maximize our resolving power while observing the relatively small *C. elegans* neuron cell bodies, we restricted our analysis to a single focal plane taken through the middle of each cell body.

Behavioral assays

The reversal frequency of individual animals was assayed as previously described but with some modifications (Zheng et al., 1999). Single young adult hermaphrodites were placed on NGM plates in the absence of food. The animals were allowed to adjust to the plates for 5 min, and the number of spontaneous reversals for each animal was counted over a 5-min period. 20 animals were tested for each genotype, and the reported scores reflect the mean number of reversals per minute. Nose-touch mechanosensation was assayed by placing young adult hermaphrodites on NGM plates with food. Individual young adult animals were allowed to collide with a human hair 10 consecutive times within a 5-min period. Activation of the reversal behavior was scored immediately after each contact with the hair stimulus, and the score was summed over the 10 trials. 30 or more animals were tested for each genotype, and the reported scores reflect the mean number of responses.

Patch clamp whole-cell recording

In vivo whole-cell recordings were performed at room temperature with an amplifier (EPC-10; HEKA) and Patchmaster software (HEKA) using a protocol described in previous studies (Wang et al., 2008; Ward et al., 2008). In brief, the head of glued worms was dissected, and the AVA neurons were exposed for patch clamp recordings in the bath solution. Recording pipettes were pulled from borosilicate glass. The pipette solution contained 115 mM K-gluconate, 25 mM KCl, 50 mM Hepes, 0.1 mM $CaCl_2$, 1 mM BAPTA, 5 mM MgATP, and 0.5 mM NaGTP (315 mOsm, pH adjusted to 7.35, with KOH). The bath solution contained 150 mM NaCl, 5 mM KCl, 5 mM $CaCl_2$, 1 mM $MgCl_2$, 15 mM Hepes, 10 mM glucose (325 mOsm, pH adjusted to 7.35, with KOH). Voltages were clamped at -70 mV. Current data were sampled at 22 kHz. 1 mM glutamate was applied for 500 ms by pressure ejection.

GST pull-downs

Complete coding sequences for the LIN-10 PTB domain, RAB-6.2, and mutant forms of RAB-6.2 were introduced into the GST expression vector pGEX-2T-GW, and either GST alone or GST-tagged proteins were expressed in *E. coli* strain BL21 and purified using glutathione–Sepharose 4B beads (GE Healthcare) as described previously (Pant et al., 2009). Bacterial cultures in 2× yeast tryptone medium were induced at an OD_{600} of 0.5 with 0.1 mM IPTG and grown overnight at 15°C. Bacteria were lysed in bacterial protein extraction reagent (B-PER; Thermo Fisher Scientific) with EDTA-free protease inhibitor cocktail (Roche). The bacterial lysate was centrifuged at 4°C at 10,000 *g* for 20 min in a rotor (SS-34; Sorval). The soluble extract was applied to a glutathione–Sepharose 4B column equilibrated with lysis buffer. The column with bound protein was washed six times thoroughly with cold STET buffer (10 mM Tris-HCl, pH 8.0, 150 mM NaCl, 1 mM EDTA, and 0.1% Tween 20). Complete coding sequences for the LIN-10 PTB domain, RAB-6.2, and its mutant forms were also introduced into the pcDNA3.1–2×HA-GW vector, and HA-tagged proteins were synthesized in vitro with the coupled transcription–translation system (TNT; Promega). For each binding experiment, in vitro synthesized HA-tagged proteins were added to the glutathione–Sepharose beads and incubated for 2 h at 4°C. After five washes in cold STET buffer and a final wash in cold STE buffer (10 mM Tris-HCl, pH 8.0, 150 mM NaCl, and 1 mM EDTA), proteins were eluted into loading buffer and separated by SDS-PAGE for Western blot analysis using anti-GST or anti-HA antibodies.

GLR-1::GFP Western blotting

Lysates were prepared from adult worms using a stainless steel dounce homogenizer (DuraGrind; Wheaton) and buffer A (50 mM Hepes, pH 7.7, 50 mM potassium acetate, 2 mM magnesium, 1 mM EDTA, and 250 mM sucrose), a protease inhibitor cocktail (Roche), and 10 mM N-ethylmaleimide. Membranes were isolated from clarified lysates by ultracentrifugation and then suspended in buffer A plus β-mercaptoethanol, SDS, and DTT. Proteins were separated from membrane lysates by SDS-PAGE, and GLR-1::GFP or actin was simultaneously detected by Western blotting using a combination of anti-GFP antibodies (GeneTex, Inc.) and antiactin antibodies (MP Biomedicals). Quantitation was performed using ImageJ, averaging normalized GLR-1::GFP/actin ratios over four independent experiments.

Yeast two-hybrid interactions

Yeast two-hybrid experiments were performed by placing the indicated bait and prey cDNA sequences into the pEG202 bait vector and pJG4-5 prey vector. The resulting plasmids were cotransformed, along with the reporter plasmid pSH18-34, into yeast strain EGY48, and transformed yeast were recovered on –His–Trp–Ura dropout plates. Resulting colonies were diluted in series on –Leu–His–Trp–Ura dropout plates to test for interactions based on growth.

Online supplemental material

Fig. S1 shows supplemental quantification data. Fig. S2 shows the localization of other synaptic proteins in *rab-6.2* mutants. Fig. S3 demonstrates that the LIN-10 PTB domain interacts with RAB-6.2 in a yeast two-hybrid assay. Fig. S4 shows that RAB-6.2 is localized to Golgi in intestinal epithelial cells. Fig. S5 shows a model for RAB-6.2 regulation of AMPAR trafficking. Online supplemental material is available at http://www.jcb .org/cgi/content/full/jcb.201104141/DC1.

References

Andersen, O.M., J. Reiche, V. Schmidt, M. Gotthardt, R. Spoelgen, J. Behlke, C.A. von Arnim, T. Breiderhoff, P. Jansen, X. Wu, et al. 2005. Neuronal sorting protein-related receptor sorLA/LR11 regulates processing of the amyloid precursor protein. *Proc. Natl. Acad. Sci. USA*. 102:13461–13466. http://dx.doi.org/10.1073/pnas.0503689102

Arighi, C.N., L.M. Hartnell, R.C. Aguilar, C.R. Haft, and J.S. Bonifacino. 2004. Role of the mammalian retromer in sorting of the cation-independent mannose 6-phosphate receptor. *J. Cell Biol.* 165:123–133. http://dx.doi .org/10.1083/jcb.200312055

Babst, M., D.J. Katzmann, W.B. Snyder, B. Wendland, and S.D. Emr. 2002. Endosome-associated complex, ESCRT-II, recruits transport machinery for protein sorting at the multivesicular body. *Dev. Cell*. 3:283–289. http://dx.doi.org/10.1016/S1534-5807(02)00219-8

Bonifacino, J.S., and J.H. Hurley. 2008. Retromer. *Curr. Opin. Cell Biol.* 20:427–436. http://dx.doi.org/10.1016/j.ceb.2008.03.009

Bonifacino, J.S., and R. Rojas. 2006. Retrograde transport from endosomes to the trans-Golgi network. *Nat. Rev. Mol. Cell Biol.* 7:568–579. http://dx.doi .org/10.1038/nrm1985

Brockie, P.J., and A.V. Maricq. 2010. In a pickle: is cornichon just relish or part of the main dish? *Neuron*. 68:1017–1019. http://dx.doi.org/10.1016/ j.neuron.2010.12.013

Burbea, M., L. Dreier, J.S. Dittman, M.E. Grunwald, and J.M. Kaplan. 2002. Ubiquitin and AP180 regulate the abundance of GLR-1 glutamate receptors at postsynaptic elements in *C. elegans. Neuron*. 35:107–120. http:// dx.doi.org/10.1016/S0896-6273(02)00749-3

Carlton, J., M. Bujny, B.J. Peter, V.M. Oorschot, A. Rutherford, H. Mellor, J. Klumperman, H.T. McMahon, and P.J. Cullen. 2004. Sorting nexin-1 mediates tubular endosome-to-TGN transport through coincidence sensing of high- curvature membranes and 3-phosphoinositides. *Curr. Biol.* 14:1791–1800. http://dx.doi.org/10.1016/j.cub.2004.09.077

Chang, H.C., and C. Rongo. 2005. Cytosolic tail sequences and subunit interactions are critical for synaptic localization of glutamate receptors. *J. Cell Sci.* 118:1945–1956. http://dx.doi.org/10.1242/jcs.02320

Chun, D.K., J.M. McEwen, M. Burbea, and J.M. Kaplan. 2008. UNC-108/Rab2 regulates postendocytic trafficking in *Caenorhabditis elegans. Mol. Biol. Cell.* 19:2682–2695. http://dx.doi.org/10.1091/mbc.E07-11-1120

Chung, H.J., J. Xia, R.H. Scannevin, X. Zhang, and R.L. Huganir. 2000. Phosphorylation of the AMPA receptor subunit GluR2 differentially regulates its interaction with PDZ domain-containing proteins. *J. Neurosci.* 20:7258–7267.

Del Nery, E., S. Miserey-Lenkei, T. Falguières, C. Nizak, L. Johannes, F. Perez, and B. Goud. 2006. Rab6A and Rab6A' GTPases play non-overlapping roles in membrane trafficking. *Traffic*. 7:394–407. http://dx.doi.org/10.1111/ j.1600-0854.2006.00395.x

Díaz, E. 2010. Regulation of AMPA receptors by transmembrane accessory proteins. *Eur. J. Neurosci.* 32:261–268. http://dx.doi.org/10.1111/j.1460-9568.2010.07357.x

Echard, A., F.J. Opdam, H.J. de Leeuw, F. Jollivet, P. Savelkoul, W. Hendriks, J. Voorberg, B. Goud, and J.A. Fransen. 2000. Alternative splicing of the human Rab6A gene generates two close but functionally different isoforms. *Mol. Biol. Cell.* 11:3819–3833.

Emtage, L., H. Chang, R. Tiver, and C. Rongo. 2009. MAGI-1 modulates AMPA receptor synaptic localization and behavioral plasticity in response to

prior experience. *PLoS ONE*. 4:e4613. http://dx.doi.org/10.1371/journal.pone.0004613

Esteban, J.A., S.H. Shi, C. Wilson, M. Nuriya, R.L. Huganir, and R. Malinow. 2003. PKA phosphorylation of AMPA receptor subunits controls synaptic trafficking underlying plasticity. *Nat. Neurosci.* 6:136–143. http://dx.doi.org/10.1038/nn997

Gerges, N.Z., D.S. Backos, and J.A. Esteban. 2004. Local control of AMPA receptor trafficking at the postsynaptic terminal by a small GTPase of the Rab family. *J. Biol. Chem.* 279:43870–43878. http://dx.doi.org/10.1074/jbc.M404982200

Glodowski, D.R., T. Wright, K. Martinowich, H.C. Chang, D. Beach, and C. Rongo. 2005. Distinct LIN-10 domains are required for its neuronal function, its epithelial function, and its synaptic localization. *Mol. Biol. Cell*. 16:1417–1426. http://dx.doi.org/10.1091/mbc.E04-10-0885

Glodowski, D.R., C.C. Chen, H. Schaefer, B.D. Grant, and C. Rongo. 2007. RAB-10 regulates glutamate receptor recycling in a cholesterol-dependent endocytosis pathway. *Mol. Biol. Cell*. 18:4387–4396. http://dx.doi.org/10.1091/mbc.E07-05-0486

Grant, B.D., and M. Sato. 2006. Intracellular trafficking. *WormBook.*:1–9.

Grunwald, M.E., J.E. Mellem, N. Strutz, A.V. Maricq, and J.M. Kaplan. 2004. Clathrin-mediated endocytosis is required for compensatory regulation of GLR-1 glutamate receptors after activity blockade. *Proc. Natl. Acad. Sci. USA*. 101:3190–3195. http://dx.doi.org/10.1073/pnas.0306156101

Hanley, J.G. 2010. Endosomal sorting of AMPA receptors in hippocampal neurons. *Biochem. Soc. Trans.* 38:460–465. http://dx.doi.org/10.1042/BST0380460

Hart, A.C., S. Sims, and J.M. Kaplan. 1995. Synaptic code for sensory modalities revealed by *C. elegans* GLR-1 glutamate receptor. *Nature*. 378:82–85. http://dx.doi.org/10.1038/378082a0

Hayashi, Y., S.H. Shi, J.A. Esteban, A. Piccini, J.C. Poncer, and R. Malinow. 2000. Driving AMPA receptors into synapses by LTP and CaMKII: requirement for GluR1 and PDZ domain interaction. *Science*. 287:2262–2267. http://dx.doi.org/10.1126/science.287.5461.2262

He, X., F. Li, W.P. Chang, and J. Tang. 2005. GGA proteins mediate the recycling pathway of memapsin 2 (BACE). *J. Biol. Chem.* 280:11696–11703. http://dx.doi.org/10.1074/jbc.M411296200

Henley, J.M., E.A. Barker, and O.O. Glebov. 2011. Routes, destinations and delays: recent advances in AMPA receptor trafficking. *Trends Neurosci.* 34:258–268. http://dx.doi.org/10.1016/j.tins.2011.02.004

Hill, K., Y. Li, M. Bennett, M. McKay, X. Zhu, J. Shern, E. Torre, J.J. Lah, A.I. Levey, and R.A. Kahn. 2003. Munc18 interacting proteins: ADP-ribosylation factor-dependent coat proteins that regulate the traffic of beta-Alzheimer's precursor protein. *J. Biol. Chem.* 278:36032–36040. http://dx.doi.org/10.1074/jbc.M301632200

Ho, A., X. Liu, and T.C. Südhof. 2008. Deletion of Mint proteins decreases amyloid production in transgenic mouse models of Alzheimer's disease. *J. Neurosci.* 28:14392–14400. http://dx.doi.org/10.1523/JNEUROSCI.2481-08.2008

Jaillais, Y., I. Fobis-Loisy, C. Miège, C. Rollin, and T. Gaude. 2006. AtSNX1 defines an endosome for auxin-carrier trafficking in *Arabidopsis*. *Nature*. 443:106–109. http://dx.doi.org/10.1038/nature05046

Jaillais, Y., M. Santambrogio, F. Rozier, I. Fobis-Loisy, C. Miège, and T. Gaude. 2007. The retromer protein VPS29 links cell polarity and organ initiation in plants. *Cell*. 130:1057–1070. http://dx.doi.org/10.1016/j.cell.2007.08.040

Jeyifous, O., C.L. Waites, C.G. Specht, S. Fujisawa, M. Schubert, E.I. Lin, J. Marshall, C. Aoki, T. de Silva, J.M. Montgomery, et al. 2009. SAP97 and CASK mediate sorting of NMDA receptors through a previously unknown secretory pathway. *Nat. Neurosci.* 12:1011–1019. http://dx.doi.org/10.1038/nn.2362

Johannes, L., and V. Popoff. 2008. Tracing the retrograde route in protein trafficking. *Cell*. 135:1175–1187. http://dx.doi.org/10.1016/j.cell.2008.12.009

Kato, A.S., M.B. Gill, M.T. Ho, H. Yu, Y. Tu, E.R. Siuda, H. Wang, Y.W. Qian, E.S. Nisenbaum, S. Tomita, and D.S. Bredt. 2010. Hippocampal AMPA receptor gating controlled by both TARP and cornichon proteins. *Neuron*. 68:1082–1096. http://dx.doi.org/10.1016/j.neuron.2010.11.026

Kessels, H.W., and R. Malinow. 2009. Synaptic AMPA receptor plasticity and behavior. *Neuron*. 61:340–350. http://dx.doi.org/10.1016/j.neuron.2009.01.015

Lee, J.H., K.F. Lau, M.S. Perkinton, C.L. Standen, S.J. Shemilt, L. Mercken, J.D. Cooper, D.M. McLoughlin, and C.C. Miller. 2003. The neuronal adaptor protein X11alpha reduces Abeta levels in the brains of Alzheimer's APPswe Tg2576 transgenic mice. *J. Biol. Chem.* 278:47025–47029. http://dx.doi.org/10.1074/jbc.M300503200

Lieu, Z.Z., and P.A. Gleeson. 2011. Endosome-to-Golgi transport pathways in physiological processes. *Histol. Histopathol.* 26:395–408.

Lu, W., and E.B. Ziff. 2005. PICK1 interacts with ABP/GRIP to regulate AMPA receptor trafficking. *Neuron*. 47:407–421. http://dx.doi.org/10.1016/j.neuron.2005.07.006

Makino, H., and R. Malinow. 2009. AMPA receptor incorporation into synapses during LTP: the role of lateral movement and exocytosis. *Neuron*. 64:381–390. http://dx.doi.org/10.1016/j.neuron.2009.08.035

Mallard, F., B.L. Tang, T. Galli, D. Tenza, A. Saint-Pol, X. Yue, C. Antony, W. Hong, B. Goud, and L. Johannes. 2002. Early/recycling endosomes-to-TGN transport involves two SNARE complexes and a Rab6 isoform. *J. Cell Biol.* 156:653–664. http://dx.doi.org/10.1083/jcb.200110081

Maricq, A.V., E. Peckol, M. Driscoll, and C.I. Bargmann. 1995. Mechanosensory signalling in *C. elegans* mediated by the GLR-1 glutamate receptor. *Nature*. 378:78–81. http://dx.doi.org/10.1038/378078a0

Mellem, J.E., P.J. Brockie, Y. Zheng, D.M. Madsen, and A.V. Maricq. 2002. Decoding of polymodal sensory stimuli by postsynaptic glutamate receptors in *C. elegans. Neuron*. 36:933–944. http://dx.doi.org/10.1016/S0896-6273(02)01088-7

Mueller, H.T., J.P. Borg, B. Margolis, and R.S. Turner. 2000. Modulation of amyloid precursor protein metabolism by X11alpha /Mint-1. A deletion analysis of protein-protein interaction domains. *J. Biol. Chem.* 275:39302–39306. http://dx.doi.org/10.1074/jbc.M008453200

Nielsen, M.S., C. Gustafsen, P. Madsen, J.R. Nyengaard, G. Hermey, O. Bakke, M. Mari, P. Schu, R. Pohlmann, A. Dennes, and C.M. Petersen. 2007. Sorting by the cytoplasmic domain of the amyloid precursor protein binding receptor SorLA. *Mol. Cell. Biol.* 27:6842–6851. http://dx.doi.org/10.1128/MCB.00815-07

Nonet, M.L., O. Saifee, H. Zhao, J.B. Rand, and L. Wei. 1998. Synaptic transmission deficits in *Caenorhabditis elegans* synaptobrevin mutants. *J. Neurosci.* 18:70–80.

Nonet, M.L., A.M. Holgado, F. Brewer, C.J. Serpe, B.A. Norbeck, J. Holleran, L. Wei, E. Hartwieg, E.M. Jorgensen, and A. Alfonso. 1999. UNC-11, a *Caenorhabditis elegans* AP180 homologue, regulates the size and protein composition of synaptic vesicles. *Mol. Biol. Cell*. 10:2343–2360.

Offe, K., S.E. Dodson, J.T. Shoemaker, J.J. Fritz, M. Gearing, A.I. Levey, and J.J. Lah. 2006. The lipoprotein receptor LR11 regulates amyloid beta production and amyloid precursor protein traffic in endosomal compartments. *J. Neurosci.* 26:1596–1603. http://dx.doi.org/10.1523/JNEUROSCI.4946-05.2006

Pan, C.L., P.D. Baum, M. Gu, E.M. Jorgensen, S.G. Clark, and G. Garriga. 2008. *C. elegans* AP-2 and retromer control Wnt signaling by regulating mig-14/Wntless. *Dev. Cell*. 14:132–139. http://dx.doi.org/10.1016/j.devcel.2007.12.001

Pant, S., M. Sharma, K. Patel, S. Caplan, C.M. Carr, and B.D. Grant. 2009. AMPH-1/Amphiphysin/Bin1 functions with RME-1/Ehd1 in endocytic recycling. *Nat. Cell Biol.* 11:1399–1410. http://dx.doi.org/10.1038/ncb1986

Park, E.C., D.R. Glodowski, and C. Rongo. 2009. The ubiquitin ligase RPM-1 and the p38 MAPK PMK-3 regulate AMPA receptor trafficking. *PLoS ONE*. 4:e4284. http://dx.doi.org/10.1371/journal.pone.0004284

Park, M., E.C. Penick, J.G. Edwards, J.A. Kauer, and M.D. Ehlers. 2004. Recycling endosomes supply AMPA receptors for LTP. *Science*. 305:1972–1975. http://dx.doi.org/10.1126/science.1102026

Passafaro, M., V. Piëch, and M. Sheng. 2001. Subunit-specific temporal and spatial patterns of AMPA receptor exocytosis in hippocampal neurons. *Nat. Neurosci.* 4:917–926. http://dx.doi.org/10.1038/nn0901-917

Payne, H.L. 2008. The role of transmembrane AMPA receptor regulatory proteins (TARPs) in neurotransmission and receptor trafficking (Review). *Mol. Membr. Biol.* 25:353–362. http://dx.doi.org/10.1080/09687680801986480

Petris, M.J., and J.F. Mercer. 1999. The Menkes protein (ATP7A; MNK) cycles via the plasma membrane both in basal and elevated extracellular copper using a C-terminal di-leucine endocytic signal. *Hum. Mol. Genet.* 8:2107–2115. http://dx.doi.org/10.1093/hmg/8.11.2107

Pfeffer, S.R. 2011. Entry at the trans-face of the Golgi. *Cold Spring Harb. Perspect. Biol.* 3. http://dx.doi.org/10.1101/cshperspect.a005272

Rojas, R., S. Kametaka, C.R. Haft, and J.S. Bonifacino. 2007. Interchangeable but essential functions of SNX1 and SNX2 in the association of retromer with endosomes and the trafficking of mannose 6-phosphate receptors. *Mol. Cell. Biol.* 27:1112–1124. http://dx.doi.org/10.1128/MCB.00156-06

Rolls, M.M., D.H. Hall, M. Victor, E.H. Stelzer, and T.A. Rapoport. 2002. Targeting of rough endoplasmic reticulum membrane proteins and ribosomes in invertebrate neurons. *Mol. Biol. Cell*. 13:1778–1791. http://dx.doi.org/10.1091/mbc.01-10-0514

Rongo, C., C.W. Whitfield, A. Rodal, S.K. Kim, and J.M. Kaplan. 1998. LIN-10 is a shared component of the polarized protein localization pathways in neurons and epithelia. *Cell*. 94:751–759. http://dx.doi.org/10.1016/S0092-8674(00)81734-1

Saito, Y., Y. Sano, R. Vassar, S. Gandy, T. Nakaya, T. Yamamoto, and T. Suzuki. 2008. X11 proteins regulate the translocation of amyloid beta-protein precursor (APP) into detergent-resistant membrane and suppress the amyloidogenic cleavage of APP by beta-site-cleaving enzyme in brain. *J. Biol. Chem.* 283:35763–35771. http://dx.doi.org/10.1074/jbc.M801353200

Sano, Y., A. Syuzo-Takabatake, T. Nakaya, Y. Saito, S. Tomita, S. Itohara, and T. Suzuki. 2006. Enhanced amyloidogenic metabolism of the amyloid beta-protein precursor in the X11L-deficient mouse brain. *J. Biol. Chem.* 281:37853–37860. http://dx.doi.org/10.1074/jbc.M609312200

Sastre, M., R.S. Turner, and E. Levy. 1998. X11 interaction with beta-amyloid precursor protein modulates its cellular stabilization and reduces amyloid beta-protein secretion. *J. Biol. Chem.* 273:22351–22357. http://dx.doi.org/10.1074/jbc.273.35.22351

Scherzer, C.R., K. Offe, M. Gearing, H.D. Rees, G. Fang, C.J. Heilman, C. Schaller, H. Bujo, A.I. Levey, and J.J. Lah. 2004. Loss of apolipoprotein E receptor LR11 in Alzheimer disease. *Arch. Neurol.* 61:1200–1205. http://dx.doi.org/10.1001/archneur.61.8.1200

Schwenk, J., N. Harmel, G. Zolles, W. Bildl, A. Kulik, B. Heimrich, O. Chisaka, P. Jonas, U. Schulte, B. Fakler, and N. Klöcker. 2009. Functional proteomics identify cornichon proteins as auxiliary subunits of AMPA receptors. *Science.* 323:1313–1319. http://dx.doi.org/10.1126/science.1167852

Shepherd, J.D., and R.L. Huganir. 2007. The cell biology of synaptic plasticity: AMPA receptor trafficking. *Annu. Rev. Cell Dev. Biol.* 23:613–643. http://dx.doi.org/10.1146/annurev.cellbio.23.090506.123516

Shewan, A.M., E.M. van Dam, S. Martin, T.B. Luen, W. Hong, N.J. Bryant, and D.E. James. 2003. GLUT4 recycles via a trans-Golgi network (TGN) subdomain enriched in Syntaxins 6 and 16 but not TGN38: involvement of an acidic targeting motif. *Mol. Biol. Cell.* 14:973–986. http://dx.doi.org/10.1091/mbc.E02-06-0315

Shi, A., L. Sun, R. Banerjee, M. Tobin, Y. Zhang, and B.D. Grant. 2009. Regulation of endosomal clathrin and retromer-mediated endosome to Golgi retrograde transport by the J-domain protein RME-8. *EMBO J.* 28:3290–3302. http://dx.doi.org/10.1038/emboj.2009.272

Shi, S., Y. Hayashi, J.A. Esteban, and R. Malinow. 2001. Subunit-specific rules governing AMPA receptor trafficking to synapses in hippocampal pyramidal neurons. *Cell.* 105:331–343. http://dx.doi.org/10.1016/S0092-8674(01)00321-X

Shi, Y., Y.H. Suh, A.D. Milstein, K. Isozaki, S.M. Schmid, K.W. Roche, and R.A. Nicoll. 2010. Functional comparison of the effects of TARPs and cornichons on AMPA receptor trafficking and gating. *Proc. Natl. Acad. Sci. USA.* 107:16315–16319. http://dx.doi.org/10.1073/pnas.1011706107

Shim, J., T. Umemura, E. Nothstein, and C. Rongo. 2004. The unfolded protein response regulates glutamate receptor export from the endoplasmic reticulum. *Mol. Biol. Cell.* 15:4818–4828. http://dx.doi.org/10.1091/mbc.E04-02-0108

Small, S.A. 2008. Retromer sorting: a pathogenic pathway in late-onset Alzheimer disease. *Arch. Neurol.* 65:323–328. http://dx.doi.org/10.1001/archneurol.2007.64

Strochlic, T.I., T.G. Setty, A. Sitaram, and C.G. Burd. 2007. Grd19/Snx3p functions as a cargo-specific adapter for retromer-dependent endocytic recycling. *J. Cell Biol.* 177:115–125. http://dx.doi.org/10.1083/jcb.200609161

Teber, I., F. Nagano, J. Kremerskothen, K. Bilbilis, B. Goud, and A. Barnekow. 2005. Rab6 interacts with the mint3 adaptor protein. *Biol. Chem.* 386: 671–677. http://dx.doi.org/10.1515/BC.2005.078

Thyrock, A., M. Stehling, D. Waschbüsch, and A. Barnekow. 2010. Characterizing the interaction between the Rab6 GTPase and Mint3 via flow cytometry based FRET analysis. *Biochem. Biophys. Res. Commun.* 396:679–683. http://dx.doi.org/10.1016/j.bbrc.2010.04.161

Turrigiano, G.G. 2008. The self-tuning neuron: synaptic scaling of excitatory synapses. *Cell.* 135:422–435. http://dx.doi.org/10.1016/j.cell.2008.10.008

Umemura, T., P. Rapp, and C. Rongo. 2005. The role of regulatory domain interactions in UNC-43 CaMKII localization and trafficking. *J. Cell Sci.* 118:3327–3338. http://dx.doi.org/10.1242/jcs.02457

Wahle, T., K. Prager, N. Raffler, C. Haass, M. Famulok, and J. Walter. 2005. GGA proteins regulate retrograde transport of BACE1 from endosomes to the trans-Golgi network. *Mol. Cell. Neurosci.* 29:453–461. http://dx.doi.org/10.1016/j.mcn.2005.03.014

Wang, R., C.S. Walker, P.J. Brockie, M.M. Francis, J.E. Mellem, D.M. Madsen, and A.V. Maricq. 2008. Evolutionary conserved role for TARPs in the gating of glutamate receptors and tuning of synaptic function. *Neuron.* 59:997–1008. http://dx.doi.org/10.1016/j.neuron.2008.07.023

Ward, A., J. Liu, Z. Feng, and X.Z. Xu. 2008. Light-sensitive neurons and channels mediate phototaxis in *C. elegans*. *Nat. Neurosci.* 11:916–922. http://dx.doi.org/10.1038/nn.2155

Whitfield, C.W., C. Bénard, T. Barnes, S. Hekimi, and S.K. Kim. 1999. Basolateral localization of the *Caenorhabditis elegans* epidermal growth factor receptor in epithelial cells by the PDZ protein LIN-10. *Mol. Biol. Cell.* 10:2087–2100.

Xie, Z., D.M. Romano, and R.E. Tanzi. 2005. RNA interference-mediated silencing of X11alpha and X11beta attenuates amyloid beta-protein levels via differential effects on beta-amyloid precursor protein processing. *J. Biol. Chem.* 280:15413–15421. http://dx.doi.org/10.1074/jbc.M414353200

Yang, P.T., M.J. Lorenowicz, M. Silhankova, D.Y. Coudreuse, M.C. Betist, and H.C. Korswagen. 2008. Wnt signaling requires retromer-dependent recycling of MIG-14/Wntless in Wnt-producing cells. *Dev. Cell.* 14:140–147. http://dx.doi.org/10.1016/j.devcel.2007.12.004

Yeo, S.C., L. Xu, J. Ren, V.J. Boulton, M.D. Wagle, C. Liu, G. Ren, P. Wong, R. Zahn, P. Sasajala, et al. 2003. Vps20p and Vta1p interact with Vps4p and function in multivesicular body sorting and endosomal transport in *Saccharomyces cerevisiae*. *J. Cell Sci.* 116:3957–3970. http://dx.doi.org/10.1242/jcs.00751

Zheng, Y., P.J. Brockie, J.E. Mellem, D.M. Madsen, and A.V. Maricq. 1999. Neuronal control of locomotion in *C. elegans* is modified by a dominant mutation in the GLR-1 ionotropic glutamate receptor. *Neuron.* 24:347–361. http://dx.doi.org/10.1016/S0896-6273(00)80849-1

Zheng, Y., J.E. Mellem, P.J. Brockie, D.M. Madsen, and A.V. Maricq. 2004. SOL-1 is a CUB-domain protein required for GLR-1 glutamate receptor function in *C. elegans*. *Nature.* 427:451–457. http://dx.doi.org/10.1038/nature02244